USE OF VISUAL DATA IN BENTHIC ENRICHMENT CLASSIFICATION

by

Michelle Simone

Submitted in partial fulfillment of the requirements
for the degree of Master of Science

at

Dalhousie University
Halifax, Nova Scotia
December 2014

DEDICATED TO

My family.

TABLE OF CONTENTS

LIST OF TABLES

LIST OF FIGURES

ABSTRACT

Artificial eutrophication continues to be a primary concern associated with aquaculture practices. In Canada, monitoring benthic health in response to organic enrichment is used to manage these impacts and maintain the desired oxic state in surface sediments. However, results of this study suggest that traditional methods using sulfide concentrations alone are unable to distinguish between oxic and anaerobic non-sulfidic conditions. This work demonstrates that the homogenization of subsamples combined with limitations of a single parameter classification resulted in 93% of hypoxic stations, defined by known biochemical and geochemical visual signatures, were being underestimated and ranked as oxic with the current sulfide based system. Sediment surface video and *in situ* sediment profile imagery (SPI) data, including a validated use of the apparent redox potential discontinuity (aRPD) as a proxy for redox state, were integrated into visual based benthic health indices. Parameters used in the indices are supported by published sensitivity studies, thus supporting the use of the visual proxies to classify benthic enrichment and define the currently underestimated hypoxic condition resulting from sulfide concentrations alone.

List of Abbreviations and Symbols Used

Abbreviation	Description
NSDFA	Nova Scotia Department of Fisheries and Aquaculture
EMP	Environmental monitoring program
SOP	Standard operating procedure
EQO	Environmental quality objective
SPI	Sediment profile imagery
ORP	Oxidation-reduction (redox) potential
Eh_{NHE}	Redox potential normalized to a hydrogen reference electrode
RPD	Redox potential discontinuity
aRPD	Apparent redox potential discontinuity
Total S^2-	Total dissolved sulfide (H_2S + HS^- + S^{2-})
RGB	Red-green-blue
spp.	Species
BHQ	Benthic health quality
OSI	Organism-sediment index
VBH	Visual benthic health index
SF	Shellfish lease
FF	Finfish lease
FF(H)	Historic finfish lease
AVS	Acid volatile sulfide

Symbol	Description	Units
E_0	Unadjusted redox potential	mV
T	Temperature	°C
Composition		
CO_2	Carbon Dioxide	
SO_4^{2-}	Sulfate	
H_2S, HS^-, S^{2-}	Reduced sulfur species or sulfide	
FeOOH	Oxidized iron minerals	
H^+	Hydrogen ions	
Fe^{2+} or Fe (II)	Ferrous Iron	
Fe (III)	Ferric Iron	
S(0)	Elemental sulfur	
FeS	Unstable amorphous iron sulfide	
FeS_2	Pyrite	
KCl	Potassium Chloride	
NO_3^-	Nitrate	
Mn	Manganese	
CH_4	Methane	
O_2	Oxygen	
Ag^+	Silver	

ACKNOWLEDGEMENTS

There are many people whom I acknowledge for helping me throughout this entire processes. First, to my supervisor Dr. Jon Grant, thank you for accepting me into your lab and mentoring me over the past two years. I have learned so much from you and I am so appreciative of all the feedback, guidance, and support you have provided me. I thank my thesis/examining committee - Dr. Peter Cranford, Dr. Stephanie Kienast, Dr. Christopher Taggart, and Dr. Douglas Wallace - for all your time, advice and encouragement throughout this project, during meetings, and at my defence.

A very special thank you goes out to Sweeney International Marine Corporation (SIMCorp) for collaborating and supporting me from the very beginning and also to Cooke Aquaculture Inc. who donated a lot of boat time and man power to my efforts. Next I would like to thank the individuals who helped me in the field and lab - Leah Lewis-McCrea, David Cook, Raymond Garland (and his crew), and of course the Grant-Lab: Francisco Bravo, Jeff Barrell, Mike Brown, Ramón Filgueira, Zeyu Zhang, and Danni Harper. The long...LONG hours in both the lab and the field would have been much longer and less enjoyable if you all weren't there to lend a hand. So again, THANK YOU! I also wish to recognize my friends and colleagues - past and present - in the Department of Oceanography. Thank you for all the encouragement, support - and most of all- the laughs, you have contributed to my experience in the best possible way.

Finally, my family - Mom, Dad, and Alexandr you guys are, above all else, the real reason I've made it this far. Your constant love and support has quickly extinguished any doubts I have had along the way and motivated me to push harder. No words will every be enough to express my gratitude or my love, so instead I dedicate this thesis to you.

CHAPTER 1

INTRODUCTION

Aquaculture, producing almost half of the global aquatic food budget, has expanded to become a vital activity in the Canadian economy (Fisheries and Oceans, 2010). However, community support continues to be divided for various reasons, including concerns for ecosystem and stock health. This often results in social conflicts during industrial development; threatening the sustainability of the practice. Sustainability in this context refers to the ability to maintain a viable economic industry without negatively affecting the equity of the environment. At the same time, sustainability considers and addresses social concerns, including those of the community and environmentalist stakeholders. Hypothetically these concerns can be, at least partially, alleviated by working within the natural resilience of the ecosystem.

Currently, the majority of marine aquaculture leases in Atlantic Canada reside in sheltered coastal environments that experience little physical mixing relative to offshore/open ocean environments. In low flow conditions, much of the excess organic material, such as feed and faecal waste, from the farms settles on the sea-floor below and near the cages. The integrative nature of the sediments, which often characterize these coastal environments, allow for the level of enrichment to be reflected in the local biological, chemical and physical structures. Organic enrichment gradients are often found in the sediments reflecting a decrease in aquaculture impacts with increasing distance from the source (Weston, 1990; Carroll et al., 2003; Karakassis et al., 2002). For this reason, most monitoring efforts focus on measuring the extent of eutrophication by classifying the level of benthic enrichment relative to baseline or reference conditions.

In Nova Scotia, where the following work was conducted, government regulators

require farms to comply with the provincial Environmental Monitoring Program (EMP) as a condition of leases and licenses issued under the *Fisheries and Coastal Resources Act*. The frequency and level of monitoring at a site depends on the previous year's enrichment classification. Primarily, this is based on the mean total dissolved sulfide concentration measured in the top 2 cm of the sediment column. Sulfide concentrations have been widely used in the literature as a cost effective measure of benthic health from which the oxic state is inferred (Wildish et al., 2001, 1999; Carroll et al., 2003; Hargrave et al., 2008; Weston, 1990; Brooks and Mahnken, 2003). However, many stakeholders, including industry and government regulators, question the accuracy and consistency of the remote sampling technique involved, as well, the applicability of the geochemical parameters being used. For this reason, my research explores the potential of using *in situ* techniques to determine whether visual data obtained with sediment profile imagery (SPI) and sediment surface video can be used as a viable alternative to the current EMP. This project was supported by Sweeney International Marine Corporation (SIMCorp), one of the leading aquaculture consulting businesses in Atlantic Canada, who had expressed particular concern surrounding the uncertainty and success of total dissolved sulfide detection.

Outline

The investigation reported here has been broken into two experiments that focus on different aspects and applications of visual data in benthic enrichment classification. Both experiments were conducted around various aquaculture leases in Nova Scotia, Canada.

- **Chapter 2** describes a validation experiment investigating the use of SPI as a tool to measure the redox state of surface sediments. More specifically, it was designed to see if the redox state could effectively be inferred from sediment column images and whether visual signatures coincided with the geochemical profiles in soft sediments.

- **Chapter 3** then investigated the use of SPI and surface video in monitoring efforts to explore the extent to which visual data can estimate the level of benthic enrichment. A Visual Benthic Health (VBH) index, based on visual parameters extracted from the image data, was developed to rank the level of organic enrichment at a given site. Current Nova Scotia Department of Fisheries and Aquaculture (NSDFA) standard operating procedures were followed to collect sediment samples alongside the visual

data collection to compare the differences in benthic health assessment. This was then used to determine if visual data could replace and/or be used to improve current practices.

The end of this document summarizes the two experimental chapters in a conclusion chapter and includes recommendations for future EMP efforts to increase the environmental and social sustainability of aquaculture in Nova Scotia. This has been presented with the assumption that the tools and analytical techniques used in this study could be extended to other geographic locations as well as be applied to other types of coastal organic enrichment assessments.

CHAPTER 2

VISUAL ASSESSMENT OF REDOX STATE IN BENTHIC SEDIMENTS

Organic matter deposits in marine sediments from activities such as aquaculture can result in undesirable phase shifts from aerobic to anaerobic dominated systems. This transition from oxic to hypoxic or anoxic states can be collectively described by the oxidation-reduction or redox state. Oxic state is achieved when the supply of oxygen exceeds or is balanced by the metabolic demands of the sediments; aerobic respiration oxidizes organic matter to CO_2 through the reduction of oxygen to water. The balance of oxidation and reduction reactions generates an electrical potential that can be measured with a platinum electrode corrected to a normal hydrogen reference electrode (Eh_{NHE}). For this reason, when the sediments are oxidized, positive potentials are measured because the pore-water has a strong tendency to accept protons from the reaction ($Eh_{NHE} \geq 0$). In contrast, negative potentials are measured in stressed conditions, for example hypoxia, where oxygen supply is surpassed by metabolic demand and organic matter breakdown is facilitated by other, less thermodynamically favourable oxidants (Berner, 1980, 1981b; Claypool and Kaplan, 1974; Curtis et al., 1977). These anaerobic processes result in an incomplete reduction of the organic compounds. To this end, the sediments where these reactions occur define the benthic redox state as reduced or reducing ($Eh_{NHE} \leq 0$). It is the transition, between positive and negative redox potentials ($Eh_{NHE} = 0$), that defines the spatial extent of the desired oxygenated state (Fenchel, 1969; Fenchel and Riedl, 1970). This 0 mV isovolt in the redoxcline is referred to as the redox potential discontinuity (RPD).

In benthic marine environments, the availability of sulfate (SO_4^{2-}) exceeds the other

major oxidants (nitrate, iron and manganese) giving it the potential to be the most important electron acceptor in the upper anaerobic zone (Thamdrup et al., 2000; Finke et al., 2007; Jørgensen, 1977). Sulfate-reducing bacteria oxidize organic compounds by reducing sulfate (SO_4^{2-}) into unstable sulfur species (H_2S and HS^-). These reduced products of sulfate reduction are collectively referred to as dissolved sulfide (S^{2-}), and are highly toxic for fauna (Grieshaber and Völkel, 1998; Bagarinao and Lantin-Olaguer, 1998; Gray et al., 2002). As well, sulfide species are thermodynamically sensitive to chemical oxidation by either dissolved oxygen or iron-oxides and hydroxides prevalent in sediments (Berner, 1980; Jørgensen, 1977). Previous works have suggested that the aerobic chemical oxidation of dissolved sulfide accounts for about 50% of total dissolved oxygen uptake in the sediments (Berner, 1979; Jørgensen, 1977). It is because of this reactivity that a region where neither oxygen nor sulfide are present in measurable concentrations ($\leq 1\mu$M) is able to form; and it is here where the Eh becomes negative (Berner, 1981a; Froelich et al., 1979; Fenchel and Riedl, 1970). In such regions of low to no dissolved oxygen, ferric oxidation becomes the dominant chemical oxidation pathway used to detoxify sulfide:

$$2FeOOH + HS^- + 3H^+ \rightarrow 2Fe^{2+} + S(0) + 4H_2O \tag{2.1}$$

where oxidized iron minerals present in the sediment react with dissolved sulfide to produce reduced iron ions and elemental sulfur. The reduced iron can then further sequester sulfide by precipitating amorphous iron sulfides or monosulfides (Jørgensen, 1977; Berner, 1980, 1979; Howarth, 1979; Berner, 1984):

$$Fe^{2+} + HS^- \rightarrow FeS + H^+ \tag{2.2}$$

The monosulfides produced are no longer toxic to fauna (Brooks and Mahnken, 2003), however, they are still thermodynamically unstable under oxidizing conditions (Jørgensen, 1977; Otero et al., 2006). The precipitates are dark grey-black in colour, contrasting the lighter oxidized sediments. Therefore a visual signature, representative of the transition from dominantly aerobic to dominantly anaerobic conditions, is formed (Rosenberg et al., 2001; Jørgensen and Fenchel, 1974; Rhoads, 1974; Pearson and Rosenberg, 1978; Lyle, 1983). Although sulfate reduction is not the first anaerobic metabolic pathway that occurs vertically in the sediment column, it is the dominant reaction (Middleburg et al., 2005;

Jørgensen, 1977; Thamdrup et al., 2000; Finke et al., 2007; Berner, 1980) and responsible for the change in sediment colour. Therefore the visual boundary, known as the apparent RPD (aRPD), has long been considered and indirect measure of the RPD (Froelich et al., 1979; Lyle, 1983; Rosenberg et al., 2001). Moreover, despite the transition from oxic to oxygen free conditions inherent to the RPD, the redox potential is not a measure of the dissolved oxygen concentration. Instead, it represents the potential for aerobic respiration relative to the other reducing pathways (Fenchel, 1969; Fenchel and Riedl, 1970).

Due to the value of this transition as an indicator of redox state, especially in response to organic loading, various observational techniques have been employed, including sediment coring and an *in situ* method known as sediment profile imagery (SPI). For example, in intertidal mudflats the depth of the RPD colour change has been measured from the voids left by removed cores (Gerwing et al., 2013). Alternatively, SPI has been used in subtidal environments. Sediment profile imagery is a technique in which a closed wedge-shaped core is inserted vertically into the sediment. An internal mirror system allows for an image of the sediment column to be obtained with an on-board camera. Image analysis is then used to extract various features from the sediments, including the depth of the aRPD and other physical-chemical properties, and biological parameters (Rhoads and Germano, 1982). Although this method was pioneered to investigate organism-sediment relations in the 1970s (Rhoads and Cande, 1971), it has since been used as a tool applied to monitoring benthic biogeochemical cycling on various temporal and spatial scales both quantitatively and qualitatively (Rhoads and Germano, 1982, 1986; Van Hoey et al., 2014; Karakassis et al., 2002; Grizzle and Penniman, 1991; Valente et al., 1992; Mulsow et al., 2006; Carlsson et al., 2012; Nilsson and Rosenberg, 1997, 2000). Variables measured from image analysis have also been combined into indices as a qualitative measure of benthic community health (Nilsson and Rosenberg, 1997; Rhoads and Germano, 1982).

Eutrophication of coastal waters is a significant concern globally (Selman et al., 2008), and regulatory agencies are interested in efficient and effective techniques for evaluating benthic health. Due to the value of inferring the desired oxic state of sediments, redox potential has been used extensively in environmental monitoring (Wildish et al., 1999, 2001; Hargrave et al., 2008; Hansen et al., 2001). The ability to resolve sedimentary biogeochemical variables, with the benefit of an undisturbed *in situ* view would be a powerful approach for benthic assessments. For this reason, an ability to use the depth of

the RPD colour change quantitatively by relating it to electrochemical measures of redox is an important step in the application of *in situ* methods such as SPI to environmental assessment.

Comparisons between the visual indicators and the chemical redox state in pore-water, measured with electrodes, have been made previously in both intertidal and subtidal sediments (Rosenberg et al., 2001; Gerwing et al., 2013). However, due to opposing conclusions in the literature and the development of new sampling techniques, a key objective of this study was to examine the accuracy of the aRPD as a proxy for the RPD in soft-bottom, subtidal environments. The aRPD was measured with an *in situ* SPI instrument and transparent acrylic cores; cores were also used for redox potential measurements. Traditionally, SPI-cameras are suspended in a large frame that settles on the sea-floor before a piston releases the wedged-housing into the sediment (Van Hoey et al., 2014; Coggan et al., 2007; Nilsson and Rosenberg, 2000; Rhoads and Germano, 1986; Rhoads, 1974). However, in this study, a customized SPI was used to passively penetrate the sediments on impact to investigate whether a minimal frame, and reduced weight, would increase the ease of operation and potentially broaden the use of SPI as a tool in both science and industry.

2.1 Materials and Methods

Samples were collected in Shelburne Harbour, Shelburne, Nova Scotia (Figure 2.1). The head of the bay is the mouth of Roseway River and narrows approximately 9 km south

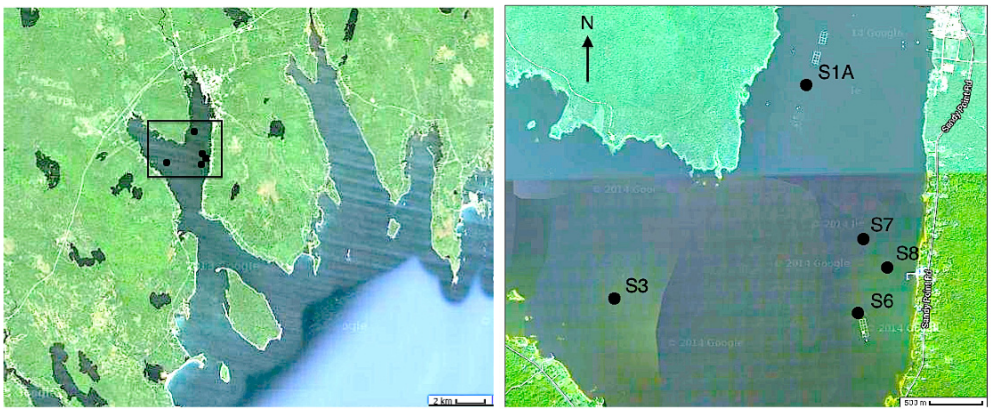

Figure 2.1: Map of Shelburne Harbour with stations labelled by name. Three inactive salmon leases are visible in the map; two north of S1A and one south of S6.

at Sandy Point where it is joined by Birchtown Bay. Further south the system widens to the larger bay and open ocean. The small town of Shelburne at the head of the harbour includes a fishing port and other commercial activity. Fish farming has been conducted in Shelburne Harbour for many years, although most sites are now fallowed. Four location were sampled in Shelburne Bay and a single location in Birchtown Bay. All stations were sampled on the same day (July 24, 2014) from different 80 m^2 areas with similar depths (13.5 $\pm$ 1.13 m) and bottom water temperatures (7.4 $\pm$ 0.3°C).

All visual and redox profiles were recovered south of the township and north of the bay terminus. Station locations were selected so both cores and SPI images would have a visually oxic sediment surface $>$2 cm and include an aRPD boundary followed by $>$2 cm of visually reduced sediments. This $>$2 cm rule was meant to allow for the redoxcline, both above and below the visual transition, to be measured in the geochemical profiles. However, the low frequency and non-random selection of site locations prevented any bay-scale spatial patterns to be resolved.

Sampling was limited to soft sediments to allow for SPI penetration and core recovery. Three inactive salmon leases are visible in the map (Figure 2.1); two north of S1A (fallowed since Sept. 2008 and July 2009; Specter and Specter, 2010) and one south of S6 (fallowed from Aug 2008 - July 2009 and then retired all operation in 2011; Milewski, 2013). Now only one active trout farm lease operates in the upper harbour approximately 100 m north of S1A (not shown).

2.1.1 Sediment Profile Imaging

At each 80 m^2 (approximately 9 x 9 m) station the SPI-camera was deployed three times (Figure 2.2) and four acrylic cores were retrieved by divers. The SPI-camera used in this study was centred on a Canon EOS Rebel T3i digital camera with an approximately 18.0 megapixel resolution. The camera was powered with internal batteries and a hot shoe flash, and was linked to the vessel via an ethernet extended USB cable allowing for remote viewing and shutter control with the Canon LiveView software on a tablet computer.

The aluminum camera housing had been lined with black felt to minimize flash bounce and the profile window, composed of bulletproof glass (15.5 x 22.5 cm), was located at the base of the pressurized housing. This was all suspended in a minimal aluminum frame (approximately 50 x 50 x 50 cm) with weighted feet to aid in stability and to increase vertical penetration depth (Figure 2.3).

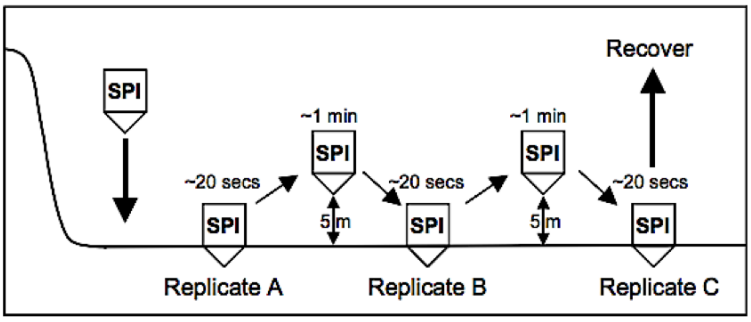

Figure 2.2: SPI benthic hopping method for triplicate sampling (MESH: Recommended operating guidelines, pp.99)

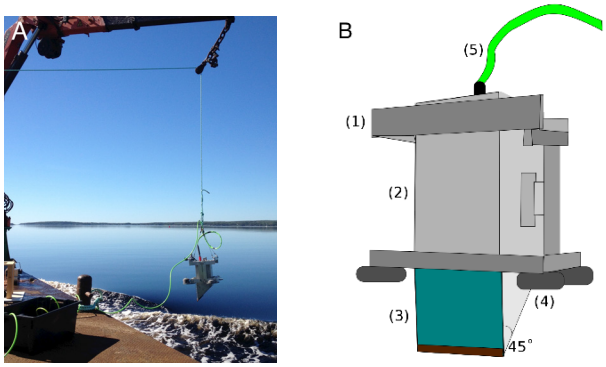

Figure 2.3: The SPI-camera set-up for sampling (A) and a component diagram (B) highlighting the (1) frame, (2) aluminium wedged-housing, (3) window, (4) weighted feet, and (5) power cable.

2.1.2 Core sampling

Four sediment cores were obtained at each station by divers to assess the mean aRPD and provide an estimate of natural spatial variability of the local redox conditions. The use of divers allowed for disturbance to the core to be minimized during collection where observations upon recovery verified undisturbed surface sediments as the absence of suspended particles in the overlying water.

Pre-marked acrylic cores were used to measure the aRPD by hand at six evenly distributed locations around the core (Figure 2.4, A). This depth was measured from the sediment surface to where the sediment colour changed from light-brown to dark-grey or black (Figure 2.5, A). A station mean aRPD was then calculated from all the cores with the standard deviation of the mean used to represent the spatial variability of the local redox state (Wildish et al., 1999).

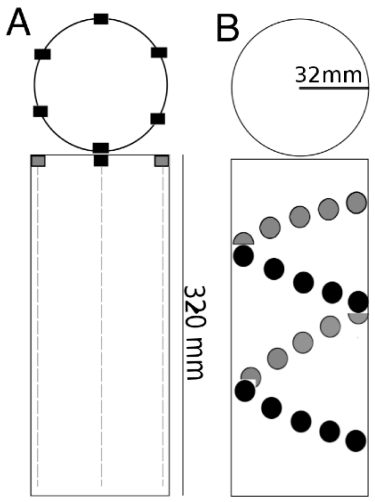

Figure 2.4: Two types of acrylic cores were used; a marked intact core (A) and a pre-drilled core (B). All cores had a 64 mm internal diameter and 320 mm height.

Redox measurement

Two of the cores were also used to measure redox potentials. These cores had been pre-drilled to allow for high resolution profiles, 15-22 measures per core, to be recovered at 0.5 cm increments up to 20 cm below the sediment surface (Figure 2.4, B). Each hole was approximately 14 mm in diameter, enough to fit an Orion 96-78NWP oxidation-reduction potential (ORP) Pt electrode with a 6 mm round sensory element, and numbered for referencing purposes when determining the depth of transitions. Immediately after cores were retrieved, the water above the sediment surface was drained and redox potentials were measured by uncovering the holes and inserting the electrode and temperature probe directly into the sediments. Measurements started from the sediment surface to avoid core collapse and the contamination of deeper sediment layers.

Values were recorded when the meter readings stabilized ($\pm$ <2 mV min^{-1}), the platinum surface was then rinsed with distilled water and blotted dry before it was used again (Wildish et al., 1999). The electrode was filled with 4 M KCl solution (Orion solution 900011) >24 hours prior to use. To ensure there was no probe drift, meter performance was assessed with ORP standard solution (Orion 967901; + 220 $\pm$ 3 mV at 25°C) immediately before and after all samples were measured. The RPD was defined after the meter readings were corrected for core temperature and normalized to the hydrogen reference solution

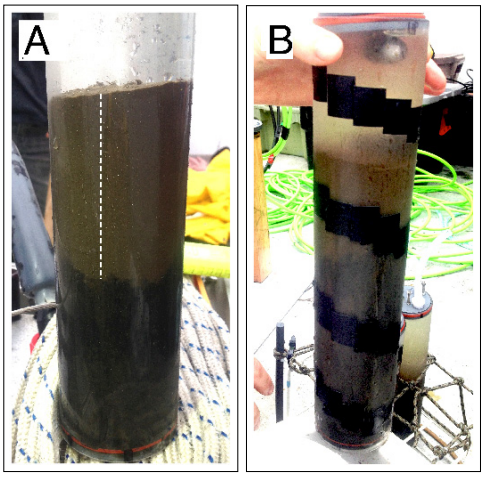

Figure 2.5: Example of an intact core (A) and a drilled core (B) with holes covered in black electrical tape retrieved from station S7. Dashed line shows what would be measured as an aRPD from the sediment surface to the colour change.

(Equation 2.3) as the depth (cm) where the redox potential was 0 mV.

$$Eh_{NHE} = E_0 + (224 - T) \tag{2.3}$$

where E_0 is the unadjusted mV reading and T is the temperature at sample depth in °C (Wildish et al., 1999). Finally, the transparent acrylic cores allowed for the visual detection of the aRPD during redox profiling, these hole numbers were recorded for each core so the corresponding redox measurements could be used to define a redox potential range for the visual transition and the depth of the visual transition could be included in the core calculated station mean aRPDs.

2.1.3 SPI image analysis

The aRPD was extracted from SPI images using Matlab^{TM}. This allowed for the isolation of the oxidized region through the manipulation of colour profiles. By converting the image into a two or three-toned grey-scale (Figure 2.6B), pixels could be defined as an RGB matrix. Two interfaces, sediment-water and aRPD, were then identified using a looped vector analysis (Figure 2.6C). The sediment-water interface was identified when $\geq$ 50% of the pixels in a vector had the RGB value of the oxidized layer and this point was marked and the loop continued with the next column. The same method was used to identify the aRPD. Once the two interfaces were defined, their distances to one another were averaged along the image width to get a single mean aRPD depth value. The mean

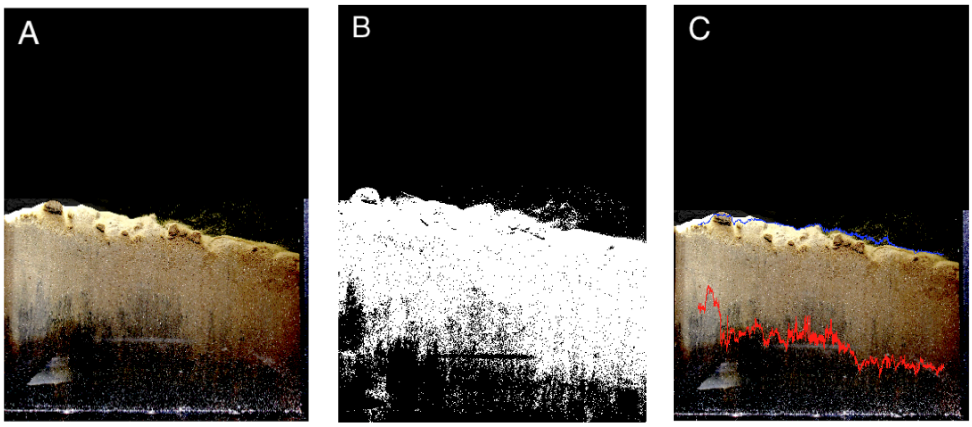

Figure 2.6: Matlab image analysis. Panel A shows the original image that is converted to two-toned grey-scale (B) from which the sediment water interface (blue line) and aRPD (red line) are detected (C). Image width is approximately 15.5 cm.

aRPDs from each image were then used to calculate a station mean aRPD (SPI-aRPD) and the standard deviation of this station mean was used to represent that natural spatial variability of the local redox conditions.

2.2 Results

All cores collected by divers and all the SPI images contained at least 2 cm of visually oxidized sediments, with grey to black sediments below. The aRPD within cores was generally observed as a solid rather than a jagged transition, although variance within the colour change, small-scale variability, was more readily seen in the higher resolution view of the SPI images.

When handling the cores for Station 8 all but one drilled core was either disturbed or lost. For this reason, Station 8 data were excluded from aRPD depth comparisons; however, the single drilled core was processed and used in the development of a millivolt range for the aRPD. Similarly, surface sediments from a single drilled core from Station 1 (Core 2) were disturbed to approximately 8 cm during profiling. However, the visual boundary had remained intact and therefore the redox potential profile was still measured and included in all analyses. The profiles from the 9 drilled cores are identified by their [Station Number].[Core Number]; for example, S1.1 and S1.2 refer to Station 1 cores 1 and 2, respectively.

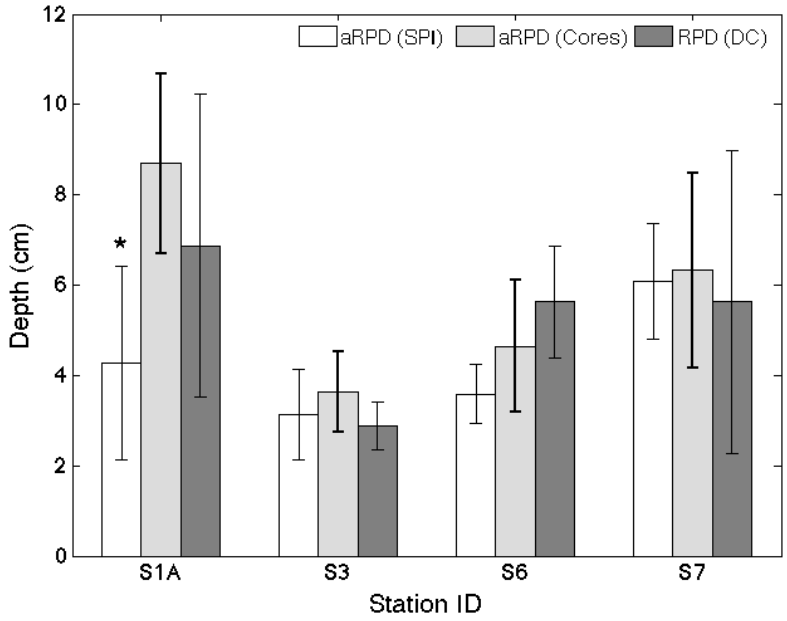

Figure 2.7: Mean aRPD (cm) calculated from SPI-images (white bars) and diver-retrieved cores (light-grey bars) alongside the mean RPD depth measured from drilled cores (dark-grey bars). Error on the mean aRPD depths represent the natural spatial variation calculated as the standard deviation among cores or SPI images.
* indicate means that fall outside the natural spatial variation of the other measures.

A comparison of the depth of the aRPD in both core types and SPI images indicates general agreement ($p>0.2$; ANOVA) at three of the four stations, with <1 cm difference between methods (Figure 2.7). In addition, standard deviations were low suggesting that random samples within an area of 80 m^2 display minimal spatial variation. This is supported by the variance in aRPD depth of diver cores, which represent about one-half of the width of SPI images, having no obvious increase in variability despite the smaller sampling area. Even though station locations were not selected to detect spatial gradients, there is an indication of increasing aRPD depth from stations 6 to 7 to 1 with decreasing distance from the inner harbour. However, this trend was not found to be substantial in the aRPDs measured from the diver retrieved cores ($p>0.05$; ANOVA), and the small sample size limits resolution of potential gradients.

Station 1 (S1A) has the deepest mean aRPD at almost 9 cm in cores, but with less than half this value in the mean aRPD depth from SPI images (Figure 2.7, $p = 0.03$; ANOVA). Station 1 was the first of the diver samples and as a result was less spatially constrained

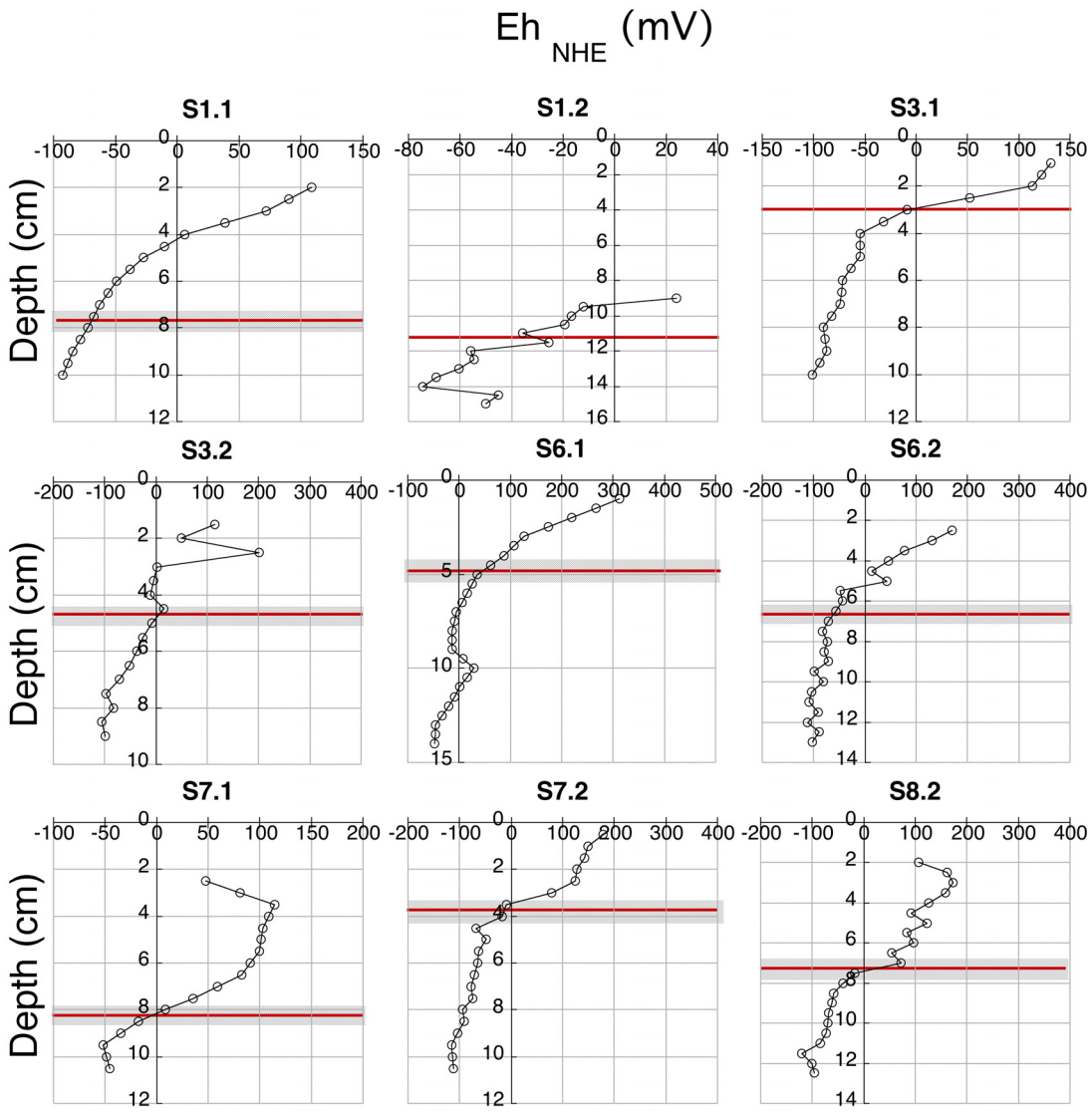

Figure 2.8: Normalized redox profiles measure from the five stations. S1, S3, S6 and S7 have two drilled cores and S8 has one. Red lines represent the depth where the apparent redox potential discontinuity (aRPD) was observed and shading shows the depth range in some cases ($\pm$0.5 cm).

than the other stations. As a consequence, S1A potentially incorporates a wider area of sampling.

Up to 22 vertical redox measurements were collected from each drilled core (Figure 2.8). The total Eh range measured in cores from oxidized surface sediments to reduced deeper sediments was from 312.5 mV to -119.8 mV, a 432.3 mV range over 9.6 $\pm$ 2.2

cm sediment column. The magnitude of the lower ranges indicate that none of the cores were strongly reducing, <-250 mV (Fenchel and Riedl, 1970). The shape of the redox profiles in most cores were typical of general exponential decline, made up of a gradual decrease in oxidized sediments to an asymptotic negative value at depth. This response was observed at stations 1, 3 (core 3.1), and 6. Cores from other stations (7, 8) had more erratic changes in redox values within the oxidized sediment, which may be typical of bioturbation or physical disturbance. The second replicate from Station 3 also displayed this pattern, indicating spatial variation in profiles within sampling locations.

The aRPD coincided with the RPD in four of the nine cores from three of the five stations. The remaining five cores had a physical separation between the geochemical and the visual discontinuity. In four of these cores the shift from positive to negative redox values occurred above the aRPD (Table 2.1). In a single case, one replicate from Station 6 (core 6.1), the aRPD colour change occurred below the 0 mV isovolt (Table 2.1). Despite this apparent variation, examination of millivolt values at the aRPD colour change suggests a close relationship between electrochemical and visual indicators of the RPD. The normalized oxidation-reduction potentials (Eh_{NHE}) measured at the aRPD boundary (red line, Figure 2.8) provided for the first time a millivolt range for the colour change to be defined, -14.94 $\pm$ 43.36 mV (mean $\pm$ S.D., n=9; Figure 2.9). Moreover, this range encompassed the 0 mV isovolt, suggesting the aRPD can be used as a proxy for RPD in soft-sediment, subtidal environments. Only three of the nine cores showed positive millivolt readings at the aRPD with the remaining six cores being low negatives (>-77 mV).

Table 2.1: Relative depths of the aRPD and RPD measured in the 9 drilled cores from the five stations.

Station #	1		3		6		7		8
Core #	1	2	1	2	1	2	1	2	2
RPD <aRPD	x	x		x		x			
RPD = aRPD			x				x	x	x
RPD >aRPD					x				

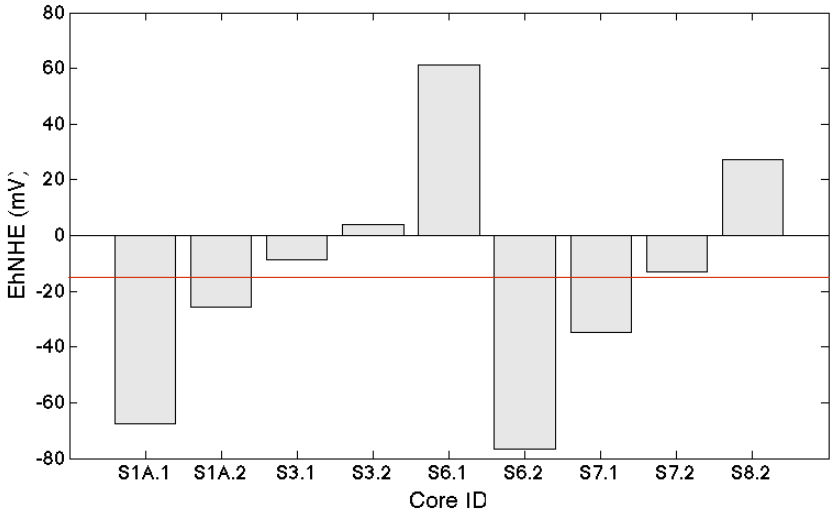

Figure 2.9: Normalized redox potentials (Eh_{NHE}) measured at the aRPD observed during drilled core analysis. Red line represents the mean isovolt (-14.94 mV).

2.3 Discussion

The use of the visual RPD as a proxy for redox state in marine sediments has been considered widely in the literature due to the importance of assessing oxic conditions as indicators of benthic health in marine sediments (Nilsson and Rosenberg, 1997; Rhoads and Germano, 1986; Gerwing et al., 2013; Rosenberg et al., 2001). Environmental impacts which result in hypoxia or anoxia are numerous, and a simple visual index of these conditions is invaluable. The aRPD is a visual representation of an integrated average of the reduction and oxidation of iron sulfide that precipitate in response to local pore-water conditions (Jørgensen, 1977; Jørgensen and Fenchel, 1974). This precipitation of darker sediments under reducing conditions (Eh_{NHE} <0 mV) does not occur immediately and therefore the colour change may lag behind the dynamics of the pore-water Eh (Jørgensen and Fenchel, 1974). This study aimed to address the uncertainty surrounding visual redox state measurements by measuring the geochemical discrepancy (RPD) and the visual transition in the same core. Limiting the physical separation between the visual and electrochemical measures allowed for a direct comparison of the RPD boundaries. In addition, a redox potential range (-14.94 $\pm$ 43.36 mV), representative of the aRPD, was able to be defined. The slight negative skew of the Eh_{NHE} values may be attributed to the presence of other oxidants being reduced before sulfate (Berner, 1980, 1981b; Claypool

and Kaplan, 1974; Curtis et al., 1977). However, because the physical discrepancy of the aRPD depth is not consistently above or below the 0 mV isovolt measured from the pre-drilled cores, no correction can be applied to the aRPD depth to improve its estimation. Regardless, the -14.94 $\pm$ 43.36 mV range narrowly straddles the Oxic B - Hypoxic A boundary defined in the enrichment nomogram by Hargrave et al. (2008), suggesting the aRPD can be applied as a sound proxy for the transition between redox states in similar subtidal environments.

Contradictory results to this study were found in Gerwing et al.'s (2013) study in the Bay of Fundy on a macrotidal mudflat. Gerwing et al. (2013) used a similar electrode to measure the RPD in sediment cores yet concluded that the aRPD could not accurately estimate the redox state of the soft sediments. This difference in results may be partially due to the sampling technique used by Gerwing et al. (2013). For example, the electrode was inserted vertically, instead of horizontally, into the sediments. In turn, they limited the depth of their measurements, and increased the potential of contaminating meter readings at deeper core depths with pore-water from above. The aRPD was then measured from the void where the core was removed. However, the difference in results is more likely attributed to the difference in sampling location; intertidal versus subtidal sediments. Pore-water turnover in intertidal surface sediments is semi-diurnal compared to the slower, and likely shallower, turnovers experienced in a subtidal bay. For this reason, the colour change used to define aRPD at low-tide, after pore-water is drained and/or mixed (Le Hir et al., 2000), is unlikely representative of conditions present when the visual profile was created.

These speculations of sampling method and location are supported with an earlier study by Rosenberg et al. (2001) that found the aRPD to be an accurate measure of RPD (R^2=0.88) in Koljöfjord, a stratified Swedish fjord. Similar to this study, Rosenberg et al. (2001) sampled in low-energy, subtidal environment with pre-drilled cores into which they inserted electrodes horizontally to compare the redox potential to the aRPD extracted from SPI images at the same sampling locations. To this end, it is hard to separate method and location influence and therefore further investigations are needed to explore the extent to which tides influence the redox conditions of intertidal surface sediments. This may be done by characterizing the visual and geochemical redox state at both high and low tide using similar techniques to those used here and in Rosenberg et al. (2001).

There are many advantages to using visual proxies in place of electrochemical readings.

For instance, in addition to providing a rapid assessment of the ecological status, *in situ* visual assessments also encompass the natural spatial variation of the redoxcline due to microniches and physical disturbance that are likely to be missed or homogenized in traditional sediment assessments (Wildish et al., 1999). Although both cores and SPI have been used to define aRPD in the past, the ability to rapidly collect multiple *in situ* images that can be digitally enhanced to reduce operator bias favours the use of SPI. Moreover, the width of SPI images relative to smaller cores would allow for a more generalized redox state to be inferred assuming that the more resolved visuals of the SPI capture a greater number of local microhabitats.

This study utilized a lighter SPI-frame model that allowed the camera housing to penetrate sediments on impact. This differs from traditional, heavy-weighted SPI camera frames that require large vessels with a winch to be able to operate the device. In order to validate the use of this new passive SPI model as a tool the mean depths of the visual boundaries were compared with the mean depths measure in the diver-retrieved cores. Results showed that only one mean SPI-aRPD depth fell outside the natural spatial variation captured by the cores (Figure 2.7), Station 1 (S1A), the rest fell within a similar site specific aRPD depth range. Based on the assumption that diver retrieved cores maintained intact sediment-water interfaces, the difference in mean aRPDs at this location would suggest that the SPI altered, or did not effectively capture, the visual redox boundary. However, it has been acknowledged that there was not as much spatial control during sampling at the first location. Upon this realization, spatial constraints were applied for the remaining three stations. Hereafter, sampling method did not appear to be an evident cause of variability. For this reason, I argue that the passive SPI model can accurately capture sediment column images from which the depth of the aRPD can be determined. In other words, the passive SPI can be used as a lighter alternative to traditional SPI designs.

Conclusion

The results of this study support the use of the aRPD as a viable proxy for RPD in soft-sediment, subtidal environments. However, due to the fact that the outcomes of this paper were based on low-flow benthic conditions, it is recommended that the visual transition be validated to ensure the redox potential range of the aRPD narrowly encompasses the 0 mV isovolt discontinuity ($\pm$ 50 mV), before the proxy is applied in more energetic environments. Nevertheless, if benthic conditions permit, SPI can then be used to rapidly

assess the ecological status of the local conditions as indicated by the redox state of the surface sediments. Sediment type still limits the application of SPI to mud or muddy-sand environments, however the lighter frame used in this study allows for the camera to be deployed from smaller vessels and operated either by hand or by winch. As a result, the passive SPI model could potential expand the use of SPI as a tool in both science and industry.

CHAPTER 3

VISUAL BASED ALTERNATIVES TO CURRENT ENVIRONMENTAL MONITORING PRACTICES

The increasing global population has depleted many of the wild fish stocks, pressuring industries to find viable and sustainable alternatives in cultured fisheries. With a four-fold increase in production over the last 20 years, Canada now ranks 26th in the world for cultured fish production, combined fin- and shellfish, and fourth when it comes to salmonids (Fisheries and Oceans, 2010). As a consequence, aquaculture has become a vital industry in many coastal and rural communities, generating over half of a billion dollars in labour income (Fisheries and Oceans, 2010). In spite of this economic success, community support continues to be divided primarily due to concerns surrounding potential impacts to the environment (Grant, 2010). In particular, many of these concerns are associated with the risk of benthic enrichment that comes from introducing organic matter, such as waste feed and fish faeces, into the system that could eventually lead to stressed oxygen conditions ($<$0.5 mg O_2 l^{-}) in the water column. To address these concerns, monitoring the enrichment effects of aquaculture practices is often used to guide management and mitigation strategies in an attempt to maintain ecosystem health.

Assessing benthic health

In assessments of eutrophic impact, evaluations of benthic conditions are often used to measure enrichment responses. This is partially due to the integrative nature of the benthic response and also to the relative stability of the sedimentary conditions, compared to those in the water column (Canfield, 1994; Berner, 1980). Faunal diversity and the

identification/quantification of tolerant species is widely used in classic benthic ecology as a measurement of ecosystem health (Pearson and Rosenberg, 1978), however this process is too time consuming and expensive to be used in a regulatory context (Wildish et al., 2001). Instead, indirect indicators of oxygenation are generally used since the oxic condition of sediments is the most desired environmental quality objective often defined in government monitoring programs (NSDFA, 2014a). More specifically, it is the identification of hypoxic or reduced conditions at the sediment surface resulting from enrichment that are used to trigger mitigation strategies.

The most frequent, and influential, geochemical property often used in monitor efforts is the concentration of total dissolved sulfide (total S^{2-}) measured in the top two centimetres of the sediment column (Wildish et al., 2001, 1999; Hargrave et al., 2008; Berner, 1981a). Total dissolved sulfide is a measure of the highly toxic end products of sulphate reduction, which in marine sediments, is the dominant metabolic pathway in the upper anaerobic zone (Thamdrup et al., 2000; Finke et al., 2007; Jørgensen, 1977). It is because this process occurs in the absence of oxygen that its products are used to define the oxygen free condition. Even though sulfide and oxygen can coexist in measurable concentrations ($>1\mu$M) (Berner, 1981a; De Wit et al., 1989), this condition highly thermodynamically unstable and the reduced sulfur are rapidly re-oxidized form oxidized sulfur species and H_2O (Berner, 1979). However, in the absence of dissolved oxygen, sulfide can accumulate in sediment pore-waters and create toxic environments absent of macrofauna (Gray et al., 2002).

In addition to, or more often in support of sulfide concentrations, redox potential is measured as a proxy commonly used to define the spatial extent of the oxidized condition (Wildish et al., 1999, 2001; Fenchel, 1969; Fenchel and Riedl, 1970). Traditionally, redox potential is measured and expressed relative to a normal hydrogen reference electrode (Eh_{NHE}) where positive values represent oxygenating conditions and negative values represent reducing conditions. In general, when oxygen concentrations in the water column are sufficient, the combination of physical and biological irrigation oxidize the surface sediments to varying depths to allow for aerobic respiration as the dominant diagenic reaction (Pearson and Rosenberg, 1978; Gray et al., 2002). Below these depths, where the concentration of oxygen is no longer sufficient, progressively less favourable electron acceptors are used to metabolize organic matter (Thamdrup et al., 2000; Finke et al., 2007;

Berner, 1981a). This transition from oxygen to other electron acceptors (NO_3^-, Mn and Fe oxides and hydroxides, SO_4^{2-}) is defined as the redoxcline, or RPD, and is traditionally measured by the rapid change from positive to negative electron potential; Eh_{NHE}= 0 mV (Fenchel and Riedl, 1970; Rosenberg et al., 2001; Gerwing et al., 2013; Wildish et al., 1999, 2001; Fenchel, 1969). This shift from dominantly aerobic to dominantly anaerobic systems therefore represents the base of the desired oxic condition.

However, known geochemical responses, to reduced conditions, have also been used to visually define the depth of the redox potential discontinuity. This is referred to as the apparent RPD (aRPD, Chapter 2; Rosenberg et al., 2001; Grizzle and Penniman, 1991). The depth of the aRPD is characterized by a colour change from light-brown (oxidized) to dark-grey or black (reduced) sediments. This visual transition forms at the base of the oxygenated region where sulfide is detoxified anaerobically with iron oxides or hydroxides present in the sediment column. This anaerobic oxidation reaction forms elemental sulfur and reduced iron ions that can then further sequester dissolved sulfide by precipitating unstable amorphous iron sulfides (FeS). These are susceptible to re-oxidition, S(0) and FeOOH, or stabilization, pyrite formation (FeS_2, Jørgensen, 1977; Berner, 1979, 1984; Howarth, 1979). These precipitates are dark-grey or black in colour, contrasting the lighter brown oxidized sediments. Even though sulfate is the dominant oxidant in the upper anaerobic zone, it is not the first electron acceptor to be used diagenetically after oxygenation (Middleburg et al., 2005; Jørgensen, 1977; Thamdrup et al., 2000; Finke et al., 2007; Berner, 1980). Therefore, the visual boundary that results from the sulfide produced is used to estimate the spatial extent of the oxygenated condition, or more accurately, the start of the anaerobic condition (Rosenberg et al., 2001; Rhoads, 1974).

Numerous tools have been used to measure the depth of the aRPD. For instance, sediment profile imagery (SPI) is a reliable technique that was pioneered in the 1970s to investigate organism-sediment relations (Rhoads and Cande, 1971). Since then it has been used for a number of related applications such as the temporal and spatial monitoring of benthic community structure after a disturbance (Rhoads and Germano, 1982, 1986; Van Hoey et al., 2014), the degree and spatial extent of organic enrichment (Karakassis et al., 2002; Grizzle and Penniman, 1991; Valente et al., 1992; Mulsow et al., 2006), and the assessment of changes in the geochemical structure of sediments (Carlsson et al., 2012; Nilsson and Rosenberg, 1997, 2000; Rosenberg et al., 2001). Traditionally SPI-cameras are suspended

in large frames that settle on the sea-floor before a piston releases a wedged-housing into the sediment (Van Hoey et al., 2014; Coggan et al., 2007; Nilsson and Rosenberg, 2000; Rhoads and Germano, 1986). The wedged core then captures an *in situ* image of the sediment column from which various biological and sedimentary features can be identified, including the aRPD. Alternatively, a lighter SPI, designed to passively penetrate the sediments on impact, was used in Chapter 2 and was able to retrieve undisturbed *in situ* sediment profiles. However, this type of subsurface sampling continues to be limited to muddy and muddy sand environments.

For qualitative purposes, Nilsson and Rosenberg (1997) developed an index that incorporated various surface and subsurface features identified from SPI profiles, including the depth of the aRPD, to generate a single benthic health quality (BHQ) score. Variable values included in the index were based on the type and extent of different faunal signatures left on and in the sediment column; higher scores were assigned to features that correlated with considerable bioturbation (Nilsson and Rosenberg, 1997). The BHQ ranges from 0 to 15 corresponding with the local level of fauna succession. Rhoads and Germano (1986) also developed an index that included the depth of the aRPD as a major parameter. They called this the Organism-Sediment Index (OSI) and it evaluated benthic habitats using the apparent RPD depth, the successional stage of macrofauna, and the presence or absence of reduced chemical species near the sediment-water interface (Rhoads and Germano, 1986). The index ranges from -10 to +11; lowest values indicate highly disturbed and degraded habitats, where methane gas bubbles form in the surface sediments, and the highest values indicate regions of mature succession with very deep oxygen penetration (Rhoads and Germano, 1986).

Sub-oxic indicators

In addition to the macrofaunal and geochemical parameters included in the BHQ and OSI, microbal activity unique to the redoxcline and transitory environments has been well studied and often considered a possible candidate for qualitatively evaluating ecosystem health (Møller et al., 1985; Preisler et al., 2007; Grant and Bathmann, 1987; Hamoutene, 2014; Hamoutene et al., 2013; Fenchel and Riedl, 1970). The strongly opposing oxygen and sulfide gradients that form the redoxcline sometimes result in an anoxic, non-sulfidic condition, where neither oxygen nor sulfide are present in measurable concentrations ($\leq$1 μM) (Berner, 1981a; Froelich et al., 1979; Fenchel and Riedl, 1970; Berner, 1980). This is

sometimes referred to as the post-oxic or sub-oxic zone. These zones form when dissolved oxygen is depleted during the complete aerobic mineralization of organic matter, that is, that oxygenation was sufficient enough to not require further mineralization from sulfate reduction (Berner, 1981a). As well, these zones can persist after the depletion of oxygen and during sulfate reduction if the sulfide produced are effectively sequestered from the pore-waters with anaerobic oxidation and precipitation of amorphous iron sulfides (Berner, 1981a). Therefore, this is the same region associated with the formation of the aRPD.

The rapid oxidation and precipitation of sulfide species results in the formation of a steep sulfide gradient. This gradient in turn provides microhabitat for sulfur-oxidizing bacteria like the mat forming *Beggiatoa spp.*(Preisler et al., 2007; Møller et al., 1985) that oxidize dissolved sulfide for the chemoautotrophic fixation of CO_2 (Nelson et al., 1986). *Beggiatoa* use this gradient to orientate themselves at the HS^-/O_2 interface (Grant and Bathmann, 1987; Preisler et al., 2007; Møller et al., 1985). For instance, Møller et al. (1985) observed the behavioural responses of the mat structure to increases in oxygen. They found that within 1 minute of exposure the *Beggiatoa* filaments coiled and reversed their orientation to reposition themselves where air saturation reached 0 %. Structurally these reversals began with the part of the filament that was in closest contact with the oxygen and therefore resulted in coils and loops. Møller et al. (1985) also explain that mat structures may vary from loose to dense depending on the slope of the saturation gradient; shallow to steep, respectively. Therefore, measuring mat thickness could act as a qualitative measure of the oxygen conditions above the sediments. Although *Beggiatoa spp.* need oxygen for filament growth, their phobic response to increased concentrations of oxygen (Møller et al., 1985) positions the mats at the sulfidic/oxic boundary. Nelson et al.'s (1986) insertion of microelectrodes into *Beggiatoa* mat formations found that only 0.6 to 6% air saturation penetrated 100 to 300 μm into the mat. Thus, the presence of the bacterial mats on the sediment surface indicate that the conditions underneath, are free of dissolved oxygen.

Furthermore, even though filaments have been found in sulfidic sediments, when the surface conditions become anoxic, *Beggiatoa* will deplete their internal nitrate reserves (NO_3^-) that they use to survive periods without access to dissolved oxygen (Nelson et al., 1986; Preisler et al., 2007). A sensitivity experiment preformed by Preisler et al. (2007) found that *Beggiatoa spp.* can last up to approximately two weeks in the complete absence

of oxygen. However, at this point they are unable to survive and the mat breaks down, becoming patchy and eventually removed completely (Brooks et al., 2004; Giles, 2008; Hamoutene, 2014; Hamoutene et al., 2013; Preisler et al., 2007). Further enrichment of such anoxic conditions can eventually deplete the local SO_4^{2-} pool and result in less diageneticially favourable organic matter breakdown, facilitated by methanogens (Berner, 1981a; Oremland and Polcin, 1982). The resulting methanic conditions have also been described as non-sulfidic, anoxic environments due to the fact that sulfide is no longer being supplied by sulfate reduction (Berner, 1981a).

Many studies have observed extensive mat coverage associated with a wide range of total dissolved sulfide concentrations averaging approximately 3000 μM or more (Hargrave, 1993; Hamoutene, 2014; Brooks and Mahnken, 2003). These environments would be defined as hypoxic using Hargrave et al.'s (2008) enrichment nomogram, $>$1500 μM, however, the same nomogram characterizes these intermediate sulfide concentrations to be associated with 0.5 mg l^{-1} of O_2, which other sensitivity studies have described as unfavourable (Møller et al., 1985; Nelson et al., 1986). In contrast, in Preisler et al. (2007), a bell curve biomass distribution was found to have peak *Beggiatoa* biomass in sub-oxic sediments with low concentrations of dissolve sulfide and no dissolved oxygen. A similar bell curve response has been observed along an enrichment gradient in Weston (1990). For instance, *Beggiatoa* was found along an entire 150 m transect extending from a fish-cage. Densest mats formed on surface sediments 30-80 m from the cage. Where patchy coverage was observed directly under and at 150 m away. The linear transect used in Weston (1990) suggests that at further distances oxygen concentrations were sufficient in the pore-waters to mineralize the relatively small deposits of organic material being supplied. Contrarily, directly below the cages where relatively large deposits of organic materials were measured, about 4 times that of the other stations, the mineralization demands of the surface sediments likely surpassed oxygenation and suffocated the *Beggiatoa spp.* Therefore his evidence suggests the intermediate conditions at 30-80 m provided an optimal environment for *Beggiatoa*.

Environmental monitoring

Environmental quality objectives are used by government regulators to define enrichment thresholds so that mitigation strategies can be employed and the desired oxygenated condition in the surface sediments can be maintained. To do this, some degree of benthic

monitoring is required annually to assess the level of ecosystem health. Total dissolved sulfide concentrations are often used to define the enrichment thresholds because of their known sensitivity to re-oxidation (Berner, 1979, 1980) and the fact that they are formed with anaerobic processes Jørgensen and Fenchel (1974); Thamdrup et al. (2000); Thamdrup and Canfield (2000); Fenchel and Riedl (1970); Berner (1979, 1980). However, because non-sulfidic anaerobic sediments ($<1\mu$M O_2 and S^{2-}) such as those found in sub-oxic and mechanic conditions, can occupy centimetre scale regions (Berner, 1980; Preisler et al., 2007), sulfide data alone would be unable to distinguish between the oxic and non-sulfidic, anoxic condition.

This study explores the use of *in situ* visual data extracted from surface video and SPI to determine whether known biochemical and geochemical sensitive parameters are able to provide a more accurate definition of ecosystem health compared to the current sulfide based classification system. A visual based benthic health index (the VBH) was developed to integrate various properties so that visual thresholds could be defined and compared to existing S^{2-} based thresholds. Finally, the limitation of sediment type on the use of SPI was considered when developing the index and therefore a second visual based classification system was developed that used surface video only (Surface Index).

3.1 Methods

Seven sites were sampled for this investigation during the Nova Scotia Department of Fisheries and Aquaculture (NSDFA) mandated summer environmental monitoring program (EMP) in 2013 and 2014 (June - October) along the south shore of Nova Scotia and Cape Breton. Data were collected around both active and inactive finfish and shellfish leases at depths shallower than 20 m. A key limitation for the use of SPI is sediment type (Coggan et al., 2007; Rhoads and Germano, 1982; Carroll et al., 2003), therefore only soft sediment (mud or muddy sand) without subsurface obstructions were selected to allow for camera penetration (>4 cm).

Sediment Profile Imagery (SPI) and Surface Video

Two sources of visual data were used in this study, sediment profile imagery (SPI) and surface video. First, surface video was used to capture two minutes of undisturbed surface conditions at each station using a georeferenced SeaViewer Sea-Drop Camera 950. This

was followed by triplicate SPI drops with a passive SPI-camera that penetrated surface sediments with its aluminum wedged-housing on impact. On-board the SPI was a Canon EOS Rebel T3i digital camera with approximately 18.0 effective megapixels and LiveView capabilities. The aluminum wedged housing was suspended in a minimal frame (50 x 50 x 50 cm) with adjustable weighted feet to aid in stability and depth of vertical penetration. Three to four images were captured at each station by 'hopping' the camera across the seabed. This required lifting the device approximately 5 m above the sediment surface and shifting it to a nearby location (within 3 m of previous image) so the camera could be lowered in undisturbed sediments. The SPI frame was fitted with backup lighting to ensure clear surveillance of the sediment surface with the LiveView setting.

Sediment analysis

After the visual data were collected, the recommended methods for monitoring organic enrichment from mariculture described in Wildish et al. (1999) were followed for sediment recovery and analysis. These are the same methods referenced in the standard operating procedures (SOPs) by the NSDFA (2014b). The sediment samples were recovered from three standard (15 x 15 x 20 cm) Ekman grab deployments at each station, and 5 cm^3 syringes were used to collect homogenized surface sediments (top 2 cm) (Wildish et al., 1999). Each syringe was filled with sediments from three different points in the grab; the first and second point collected 2 cm each and the third collected 1cm. This was done twice per grab; 5 cm^3 was used to measure porosity and organic matter content and 5 cm^3 was used to measure redox potential and total S^{2-} concentration.

Sediment samples were analysed in the laboratory for porosity, percent organic matter, redox potential, and total dissolved sulfide (S^{2-}) concentration. For management purposes, the porosity and organic matter are expressed relative to the reference stations included in the EMP sampling, and were measured by drying (60°C) and then combusting sediment samples (490°C) (NSDFA, 2014b). Redox potential, measured with a platinum reference electrode (Orion 96-78NWP) with resulting potentials expressed in millivolts (Wildish et al., 1999), is used as an 'internal data check' for total S^{2-} concentration using the empirical relationship from Hargrave (2010). The total S^{2-} concentration was the classifying parameter used to define the level of enrichment as oxic, hypoxic, or anoxic (Hargrave et al., 2008). This was measured by inserting an Ag^{+}/S^{2-} combination electrode (Orion 96-16BNWP) attached to a meter calibrated to a five-point sodium sulfide standard curve

into a slurry of sediments and sulfide anti-oxidant buffer (Wildish et al., 1999). Specifics of these methods can be found in the NSDFA SOPs 2014b, Wildish et al. (1999) technical report, and/or Appendix A of this document.

3.2 Development and use of the Visual Benthic Health (VBH) index

The Visual Benthic Health (VBH) index was developed here and used to classify the level of enrichment at each station. This index was designed specifically from features found in SPI and surface video data. Its use allows for the incorporation of biological and geochemical cues that have been identified both on and below the sediment surface. Weightings of the different parameters have been adjusted to follow the relative values assigned in existing indices, Benthic Health Quality (BHQ, Nilsson and Rosenberg, 1997) and the Organism Sediment Index (OSI, Rhoads and Germano, 1986), with the addition of features frequently seen (i.e., organic debris, *Beggiatoa*, and specific epifaunal groups). The index ranges from 14 to -7 (22 point range) with the most impacted stations found in the lower ranges.

A: Infauna

All parameters in this section have positive values that are issued on a presence/absence basis. One point was assigned for fauna being both sensitive to hypoxic effects that inhibits respiration, and to toxic effects of total S^{2-} from sulfate reduction (Gray et al., 2002). The other point was assigned for infauna facilitating bioirrigation and/or bioturbation through respiration and feeding activities (Rhoads, 1974). Three different parameters were included in this section to incorporate a level of community diversity in the index.

Tubes/siphons

Presence of tubes/siphons in surface video and/or SPI sediment profiles were considered. Surface video quality was found limiting with regards to the resolution of fine-scale surface details such as tubes and siphons. For this reason, expulsion from siphon-holes captured in the videos counted as a visual cue in place of a physical structure. Tube dwellers were most often identified in SPI profiles by subsurface or above surface casts (Figure 3.1 A).

Table 3.1: Index values to calculate the Visual Benthic Health (VBH) Index. $VBH = \Sigma A + \Sigma B + C + \Sigma D + E + F$ where A are infaunal features, B are epifaunal features, C is percent cover of *Beggiatoa spp.* mats calculated from surface video, D are cage fouling deposits, E is the presence of outgassing, and F is the mean depth of the aRPD calculated from SPI images. All variables in A, B, D and E can be identified in surface video and/or SPI images.

	Feature	Value
A	**Infauna**	
	Tubes	2
	Feeding pit/mound	2
	Burrows	2
B	**Epifauna**	
	Echinoderms	1
	Benthic fish	1
	Epibenthic crustaceans	1
C	**Beggiatoa (% cover)**	
	0	0
	1 - 29	-0.5
	30 - 59	-1
	60+	-2
D	**Cage falloff**	
	Shell debris	-1
	Organic debris	-1
E	**Outgassing**	
	Gas bubbles	-2
F	**Mean aRPD (cm)**	
	0	0
	<1	1
	1 <x <2	2
	2 <x <3	3
	3 <x <5	4
	>5	5

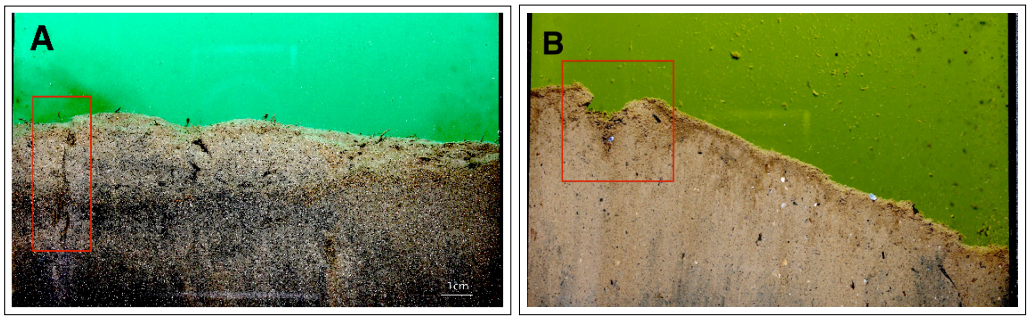

Figure 3.1: Tube structures below and above sediment surface (A) and feeding pit (B) captured in an SPI images. Width of profile is approx. 15.5 cm.

Feeding pit/mound

Feeding pits/mounds were also considered. These structures were identified in both the surface video and SPI images (Figure 3.1 B).

Burrows

Burrows were also included in the index. These were easily identified in surface videos as large holes (Figure 3.2; A) or in SPI images as tunnels and/or oxic voids at depth (Figure 3.2; B).

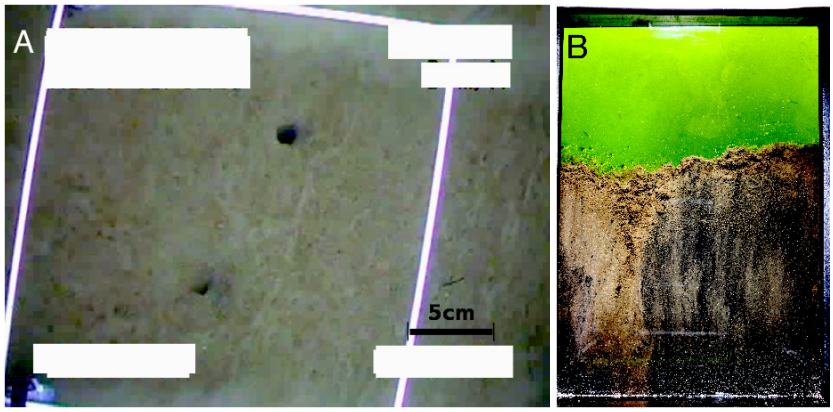

Figure 3.2: Burrows captured in surface video (A) and sediment profile (B). SPI image is approximately 15.5 cm wide.

B: Epifauna

All parameters in this section had positive values that were assigned based on the same presence/absence identification as the infauna. Again, three different parameters were

included to allow for the incorporation of community diversity. Echinoderms, benthic fish, and crustaceans were chosen because they were the most observed epifaunal groups around the farms.

Echinoderms

Echinoderms were frequently captured in surface videos in both oxic and hypoxic conditions (Figure 3.3). One point was assigned as the echinoderms provided evidence that the water just above the sediment surface was able to satisfy their respiratory needs (Gray et al., 2002) also, their motility would to disturb bacterial mats that may otherwise impede pore-water exchange.

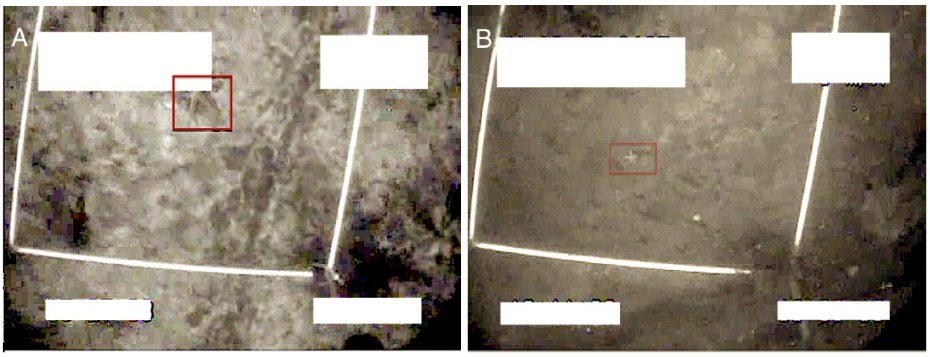

Figure 3.3: Echinoderms captured with surface video in a visually hypoxic (A) and a visually oxic (B) environment. Frame is 25 x 25 cm.

Benthic fish

Hypoxic conditions in near-bottom waters cause an avoidance response of benthic fish (Bagarinao and Lantin-Olaguer, 1998; Gray et al., 2002) and therefore the presence of these individuals has been included in the index as a positive indicator of benthic health. However, due to their fleeting nature they were not always captured in the surface videos, therefore their presence is acknowledged but not over weighted (+1 point).

Epibenthic Crustaceans

Epifaunal crustaceans (mainly crabs) were also valued in the index. Even though they are burrowing animals, they are also motile and unless captured in burrows their presence on the surface could be a result of them grazing near-by environments. For this reason only one point versus the normal infaunal two points was assigned.

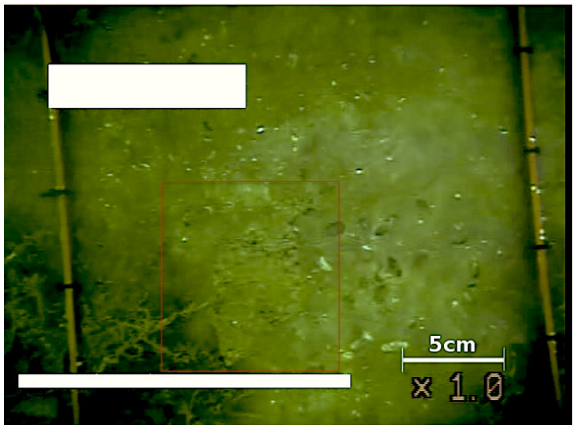

Figure 3.4: Benthic fish captured in surface video.

C: Beggiatoa spp. (% cover)

Although no genus level identifications were made on the bacterial mats, the description of shallow sulfur oxidizing *Beggiatoa* species documented from coastal sediments in Nova Scotia (Grant and Bathmann, 1987) identify the same structures observed in the study sites. For this reason, *Beggiatoa* has been used as the nomenclature of all observed benthic mats of similar morphology. *Beggiatoa* mat coverage has been assigned negative values in the index because of its dependence on sulfide for biochemical processes (Preisler et al., 2007; Nelson et al., 1986) and their rapid, phobic response to oxygen (Møller et al., 1985). Even though *Beggiatoa* was also captured in some of the SPI profiles, percent cover was determined from surface video only. Percent cover was calculated from up to six screen shots that were overlaid with a 25-point grid. After a binary presence/absence identification at the 25 points in each shot, an average was calculated to represent the extent of mat coverage for the station. Four degrees of cover were considered in the index to represent the complete range of the bell curve response *Beggiatoa* has to varying dissolved oxygen and sulfide concentrations; 0 %, 1-29%, 30-59% and >60%. The same three ranges >0%, representing low, intermediate, and extensive mat coverage, that were used in Hamoutene (2014) to evaluate spatial coverage of *Beggiatoa spp.* around finfish aquaculture sites in Newfoundland, was also used here.

Theoretically, when *Beggiatoa* is exposed to increasingly hypoxic conditions (decreasing levels of dissolved oxygen) mat coverage will expand from <30% to extensive cover (>60%; Hamoutene, 2014; Hamoutene et al., 2013; Hargrave, 1993; Brooks and Mahnken, 2003; Bertics and Ziebis, 2010). However, when exposed to increasingly anoxic conditions

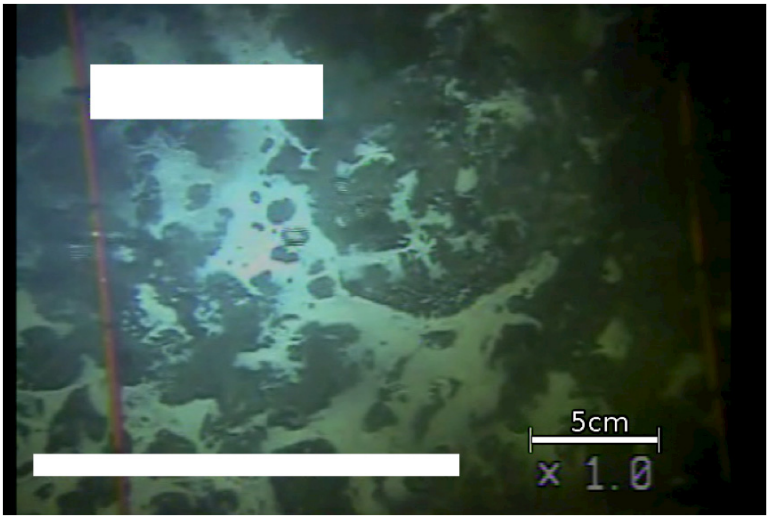

Figure 3.5: *Beggiatoa spp.* mat with 30-59% spatial coverage.

(increasing levels of dissolved sulfide and no dissolved oxygen) *Beggiatoa* are also expected to respond (Hamoutene, 2014; Hamoutene et al., 2013; Weston, 1990). This is because, even though *Beggiatoa spp.* have been found in sulfidic regions, they generally avoid this zone as they can only survive without access to oxygen for approximately two weeks (Preisler et al., 2007). Therefore low to no mat coverage can also be an indication of anoxia (Brooks et al., 2004; Giles, 2008; Hamoutene, 2014; Hamoutene et al., 2013; Weston, 1990). This response has been considered in the VBH index and valued at -3 points. It was identified as low to no mat coverage ($<$30 %) in the surface video and a 0 cm aRPD in all the depth profiles where the $>$0 cm apparent RPD was used to delineate low mat coverage as a result of anoxia.

D: Cage falloff

This variable was included to recognize the potential impacts of fish-cage fouling. For a station to be considered in this section, shell and/or organic debris (i.e. excess feed or faecal pellets) was required to be identified in the surface video and in at least 2 of the 3 SPI images (Figure 3.6). Excessive debris fouling was valued negatively in the index, as it would alter the effective grain size of the surface sediments and could significantly alter benthic biophysical processes, such as colonization and/or burrowing, from the pre-farming conditions. Moreover, soft sediments influenced by sustained organic matter on or below the sediment surface could result in long-term anaerobic metabolic processes that may retard recovery and/or sustain undesirable benthic conditions after sources (i.e., farming)

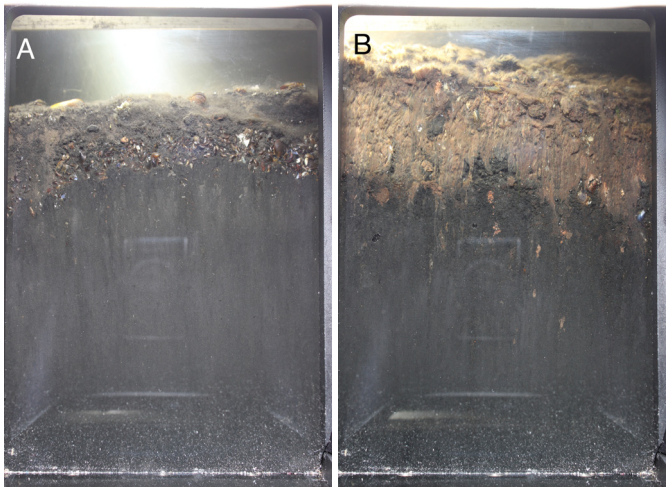

Figure 3.6: Example of what would be considered excessive shell (A) and organic (B) debris fouling in SPI images if repeated in at least one other depth profile and surface video at the same station. SPI images are approximately 15.5 cm wide.

have been removed (Berner, 1979; Canfield, 1994).

E: Outgassing

The presence of outgassing, identified in, or coming from, the sediment was assigned negative two points. One of these points was assigned because dissolved oxygen would be absent if the reduced gases were able to accumulate or to be formed in the first place and the second point was given because the accumulated gases indicated polluted conditions (Mar; Berner, 1981a; Oremland and Polcin, 1982; Hargrave et al., 2008). In surface

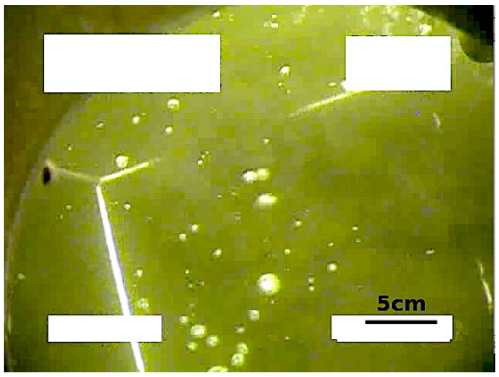

Figure 3.7: Out-gassing captured by surface video after frame contacted the sediment surface.

videos, out-gassing was often identified on the descent and/or on frame impact (Figure

3.7). Subsurface vesicles have been described in the literature (Boudreau et al., 2005) and therefore may also be captured and identified in SPI images; however, no subsurface vesicles were observed in this study.

F: Mean aRPD (cm)

Positive values (up to 5 points) were assigned based on the depth of the mean aRPD at a station. The five depth ranges considered were valued based on a generalized scaling of the aRPD distributions from both the OSI and BHQ index, where transitions within the top two centimetres are weighted more than deeper transitions. This is because benthic communities are able to reach mature succession within centimetres of the sediment surface, and any transitions deeper than this are relatively less significant in terms of successional stage (Pearson and Rosenberg, 1978; Rhoads, 1974).

Images were processed in Matlab to isolate the oxidized sediments from the water column and the reduced sediments. By converting the images into a two- to three-toned grey-scale matrix (Figure 3.8 B) from which RGB values were used to identify the surface and aRPD boundary (Figure 3.8 C). The distance between these two boundaries was calculated for each pixel-column across the image width and then averaged and divided by the image width to get an image mean aRPD depth. Station means were defined as the average of all image means calculated at the station.

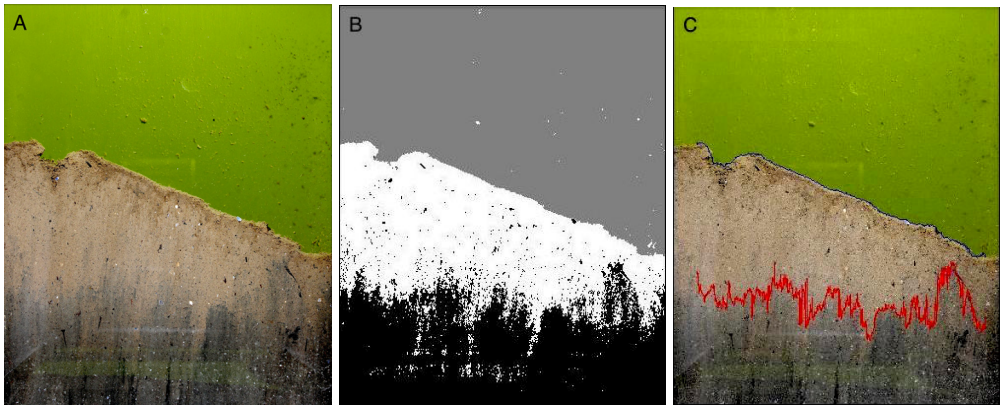

Figure 3.8: Example of the Matlab image analysis of an original image (A) converted to a three-toned grey-scale (B) from which the sediment water interface (blue line) and aRPD (red line) are detected (C). Image width is approximately 15.5 cm.

Surface Index

The limitation of sediment type on SPI prompted the development of an alternative to the VBH index that uses surface video data only. The VBH was adjusted for the exclusion of SPI data; therefore, cage falloff (section D) and mean aRPD (section F) were removed from the overall index score because the impacts of excessive deposited cage fouling were unable to be determined in surface video alone and no vertical profiles were collected for aRPD calculations. This adjusted index, the Surface Index, has a 15 point range (9 to -5) from which enrichment classifications are inferred. The same anoxic *Beggiatoa* response (-3 points) was considered in this index, but instead of a 0 cm aRPD and low to no mat coverage ($<$30%) used in the VBH, outgassing and low to no mat coverage were used in the Surface Index.

3.3 Results

A total of 37 stations from the seven sites in Nova Scotia had complete visual data sets coupled with grab sample data (Table 3.2 and 3.3). The majority of sediment samples had total S^{2-} concentrations $<$1500 μM and redox potentials ranging from -205 to 324 mV. Porosity and organic matter measures were unique to each site, but in general the SPI design limitations restricted its use in sediment with $>$35% porosity. Bottom temperatures were also measured at each station with a RBRduo profiler.

Table 3.2: Site data summary including aquaculture type (SF = shellfish, FF = finfish, H = historic or inactive leases) and number of stations at each site. Depth, temperature, and visual based index scores for with and without SPI data, VBH and Surface Index respectively, are presented as site means (min, max); n=37.

Site name	Aquaculture type	Number of stations	Depth (m)	Temperature (°C)	VBH	Surface Index
Site A	SF	14	18.1 (16.3, 19.6)	15.0 (14.6, 15.4)	3.1 (-3.0, 10.0)	1.6 (-2.0, 5.0)
Site B	FF (H)	4	10.3 (9.3, 10.7)	6.4 (6.3, 6.5)	2.8 (-6, 10.0)	1.6 (-4.0, 5.0)
Site C	FF (H)	6	11.0 (7.2, 13.2)	-	6.0 (2.5, 9.0)	3.0 (1.0, 5.5)
Site D	FF (H)	1	11.2	6.7	-2.0	-2.0
Site E	FF	3	11.4 (4.8, 18.7)	7.2 (2.8, 11.5)	-1.0 (-6.0, 8.0)	-0.5 (-4.0, 3.0)
Site F	FF	2	18.8 (18.7, 18.9)	5.7 (5.6, 5.7)	-1.5 (0.0, 3.0)	0.0 (0.0, 0.0)
Site G	FF	7	14.0 (13.3, 15.2)	8.2 (7.8, 8.8)	6.1 (-2.0, 10.0)	2.7 (-1.0, 5.0)

Table 3.3: Grab data summary for each site. Total dissolved sulfide concentrations, redox potential, porosity, and organic matter are presented as site means (min, max); n=111. * indicate data submitted to the NSDFA for summer EMPs.

Site names	Number of grabs	Total S^{2-} (μM)	Eh_{NHE} (mV)	Porosity (%)	Organic matter (%)
Site A*	42	184.3 (1.7, 740.6)	-105.5 (-204.9, 102.4)	70.9 (34.7, 86.1)	10.2 (4.2, 15.5)
Site B*	12	1073.8 (41.8, 8660.0)	-69.8 (-181.8, 65.9)	72.6 (67.8, 76.6)	17.5 (12.3, 27.9)
Site C*	18	260.5 (30.6, 1070.0)	-37.9 (-154.7, 93.2)	80.1 (76.0, 84.8)	21.9 (18.6, 31.9)
Site D*	3	1197.7 (687.0, 2160.0)	-150.0 (-166.4, -133.7)	83.2 (79.6, 85.9)	26.2 (21.1, 31.0)
Site E*	9	1048.9 (369.0, 1980.0)	-107.3 (-147.6, -54.9)	80.0 (73.2, 86.0)	14.5 (8.7, 18.7)
Site F*	6	1017.2 (597.0, 1490.0)	-126.1 (-135.8, -113.1)	47.9 (40.7, 59.4)	9.0 (6.3, 15.3)
Site G	21	532.4 (107.0, 3360.0)	125.7 (-115.5, 324.2)	80.6 (76.2, 83.2)	20.1 (17.4, 21.4)

3.3.1 Analysis of Visual Benthic Health index

The visual benthic health index included two sub-oxic formations, (1) the upper boundary of the sulfidic zone defined as the depth of the visual redox boundary (aRPD) and (2) the horizontal spatial extent of *Beggiatoa* mat coverage on the sediment surface. These were used in combination with the other biological and geochemical variables to define enrichment thresholds. Only 32.5% of stations had a mean aRPD in the intermediate depth ranges (>0 - 5 cm), meaning the remaining stations had either >5 cm deep (35%) or no (0 cm; 32.5%) aRPD (Figure 3.9, A). Figure 3.9 (B) shows a general trend of decreasing enrichment with an increasing aRPD depth, for instance all aRPDs >5 cm are coupled with oxic rankings. This reflects a well documented enrichment response most notably described by Pearson and Rosenberg (1978) in a generalized model of succession,

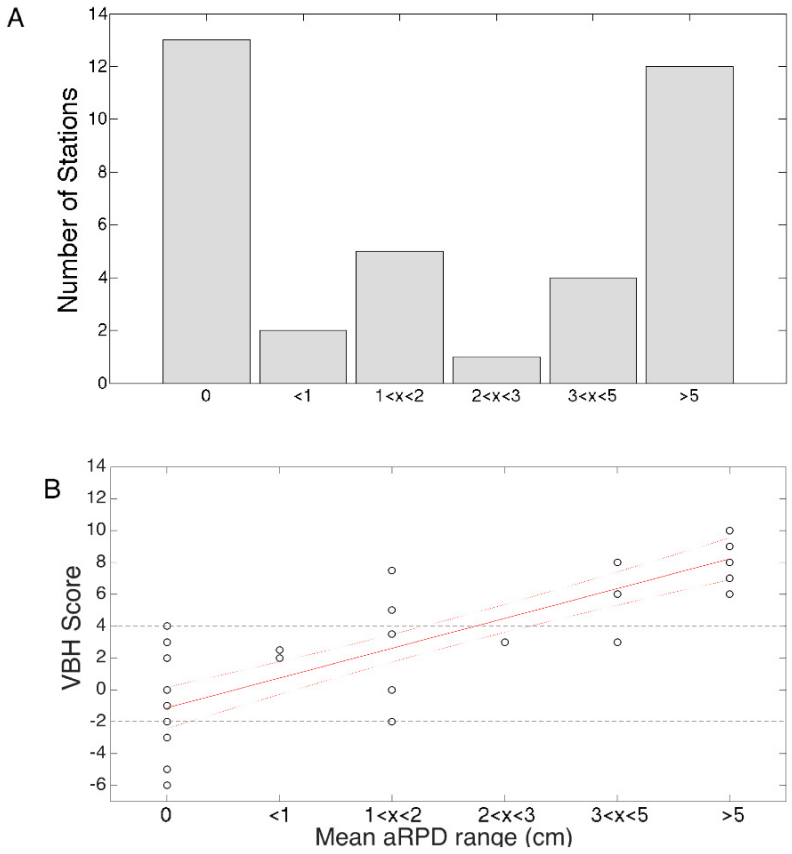

Figure 3.9: Frequency of mean aRPD ranges in cm (A) and the distribution of VBH index values in each depth range (B) for the 37 stations. Horizontal dashed lines represent the upper and lower hypoxic enrichment thresholds. Regression line (red line) with 95% confidence intervals: $y = 1.872x - 1.131$; $R^2 = 0.725$.

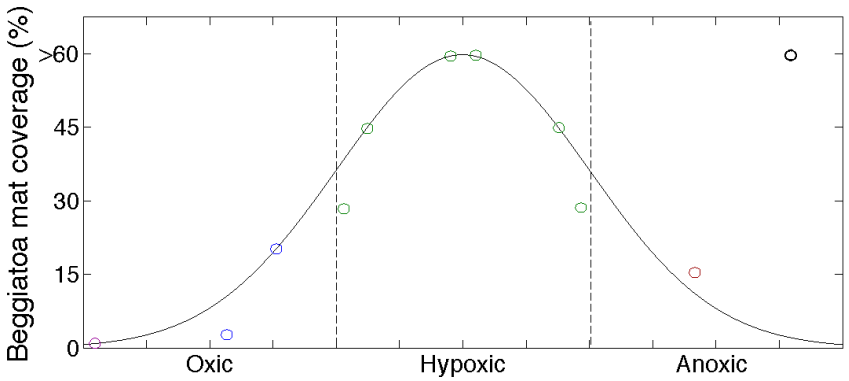

Figure 3.10: *Beggiatoa* mat coverage (%) expected curve, based on biomass distributions in Preisler et al. (2007), and observed scenarios (circular markers) for each major enrichment category ($R^2 = 0.66$). Observed enrichment classifications were determined using coupled visual data (VBH) and colours were used to group together the four major scenarios (1 - red, 2 - green, 3 - maroon, 4 - blue). A single outlier scenario was observed, $>$60% mat coverage and anoxic ranking (black).

with approximately 73% of the total VBH score being explained by the aRPD depth range. However, Figure 3.9 also shows how enrichment classifications can vary when the redox boundary is shallow, with the remaining 27% variability being attributed to the relative abundance of the other index variables. Therefore, VBH multi-parameter approach, including both positive and negative values, allows for more enrichment categories to be classified at each aRPD depth range, resulting in more diverse classifications.

Four general scenarios have been defined within the four *Beggiatoa* coverage ranges using known behavioural responses of the mat structure to sulfide and dissolved oxygen gradients (Figure 3.10). The first scenario represents a stable sulfuretum present at the sediment-water interface, characterized by low to no mat coverage ($<$30%; Figure 3.10, red marker; Weston, 1990; Hamoutene, 2014). At this stage of enrichment, *Beggiatoa* would have depleted their internal nitrate reserve (approximately 2 weeks; Preisler et al., 2007), causing the structural mat to break down. The second scenario reflects the coverage expected under varying degrees sub-oxia (Figure 3.10, green markers; Preisler et al., 2007; Weston, 1990). Scenario three can be described by the response of *Beggiatoa* to oxic conditions when dissolved oxygen concentrations force them to migrate down into the sediments (Figure 3.10, maroon marker; Møller et al., 1985; Preisler et al., 2007). The final scenario, four, considers the complex geochemical zonation patterns in sediments resulting from bioturbation activities that can result in the presence of microniches (oxidized and

reduced) Bertics and Ziebis (2010). For instance, under oxic conditions, microniches of reduced sediments reaching the surface have been found associated with low levels of *Beggiatoa* coverage (Figure 3.10, blue markers; Bertics and Ziebis, 2010).

All four scenarios were expressed to some degree in the data set. However, an additional scenario characterized by extensive mat coverage (>60%) in anoxic conditions was observed at three of the stations (one from each: Site E, Site B, and Site A; outlier scenario in Figure 3.10). The inclusion of the other negative parameters in the index, such as outgassing and excess organic matter, forced these three stations into the anoxic category. Even though this scenario does not fall on the expected *Beggiatoa* response curve (Figure 3.10), it is not unlikely. In Preisler et al. (2007), they described the ability of *Beggiatoa spp.* to tolerate toxic environments and survive for approximately two weeks in the absence of oxygen by living off their nitrate reserves. The enrichment ranking assigned to these stations, by the VBH, was therefore due to the inclusion of the other index parameters. In other words, the VBH was able to identify a level of enrichment at these three stations that would have been underestimated, with respect to the other parameters, if *Beggiatoa* data was considered alone.

3.3.2 Differences in classification

To explore the extent to which total S^{2-} concentrations alone can classify the level of benthic enrichment, sulfide data was considered relative to the more comprehensive *in situ* visual data integrated in the VBH index. Figure 3.11 shows the frequency distributions of the VBH index scores and total S^{2-} concentrations relative to the major enrichment category (oxic, hypoxic, and anoxic) thresholds. These thresholds were maintained from the enrichment nomogram in Hargrave et al. (2008) for the S^{2-} based system, and defined in the visual based system by scaling the 22 point index range to the definitions of enrichment in Hargrave et al. (2008) (dashed vertical lines). The stations appear to be well distributed across the entire VBH index range with resolution around the upper and lower hypoxic thresholds, opposed to the sulfide based distribution that appears to be heavily skewed to low concentrations (<1000 μM). Figure 3.11 shows 46% of the 37 stations being classified as oxic using the VBH relative to the 91% of grabs classified as oxic using the sulfide concentration.

In order to consider these differences further, the 37 stations were assigned two enrichment rankings ranging from 1-5 (oxic-anoxic); one based on the mean total S^{2-}

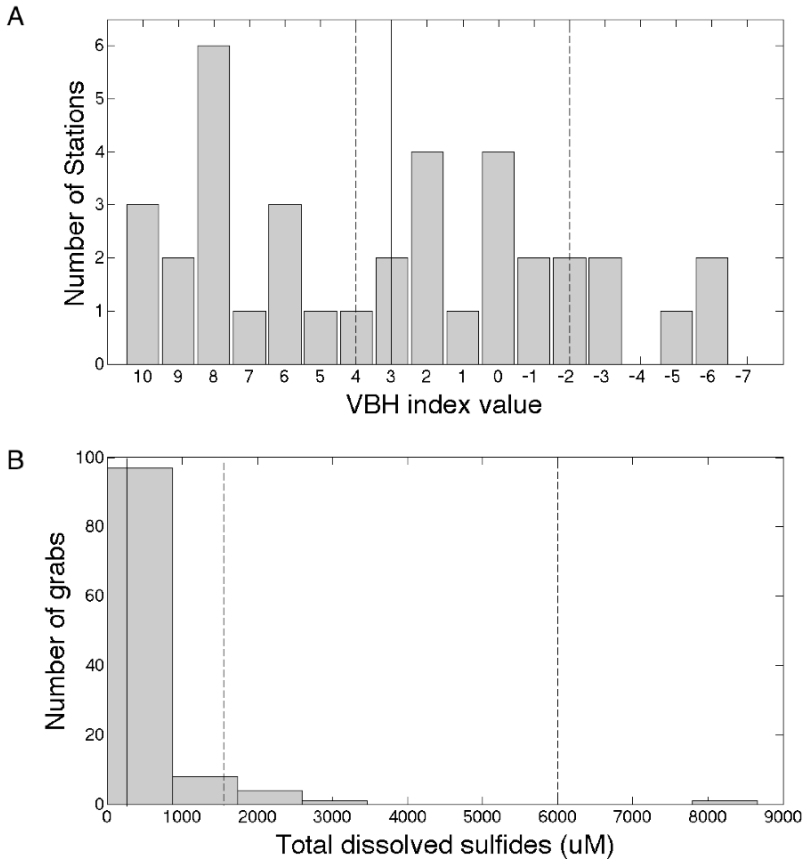

Figure 3.11: Frequency distributions of visual benthic health index values (A) and total S^{2-} concentrations (B) from the 37 stations. Index values are presented per station (n=37) and sulfide concentrations are presented per grab (3 per station; n=111). Solid vertical lines in A and B represent the median values and the dashed vertical lines represent the upper and lower hypoxic enrichment thresholds.

concentration and one based on the VBH index score (Table 3.4). Residuals were then calculated to determine how often the two classification systems agreed on the level of enrichment at a station, and how often and to what degree they did not. Subtracting the sulfide enrichment ranking from the VBH ranking resulted in positive values when the VBH ranked a station at a higher enrichment category than the sulfide data and negative values when the VBH ranked a station lower than the sulfide data.

Residual data indicate that only 12 out of the 37 stations were ranked at the same level of enrichment, all of which were classified as Oxic A (Figure 3.12). The remaining 25 stations had positive residuals, suggesting sulfide data underestimated the level of enrichment relative to visual data at 68% of stations when conditions appeared to be

Table 3.4: Total dissolved sulfide concentration distributions relative to Hargrave et al. (2008) nomogram for zonation. Visual benthic health (VBH) and Surface Index values have been scaled to the same five benthic organic enrichment groupings.

Classification	Oxic A (1)	Oxic B (2)	Hypoxic A (3)	Hypoxic B (4)	Anoxic (5)
Sulfide (μM)	[<750]	[750 <1500]	[1500 <3000]	[3000 <6000]	[>6000]
VBH	14 to 7	<7 to 4	<4 to 2	<2 to -2	<-2 to -7
Surface Index	9 to 4	<4 to 2	<2 to 0	<0 to -2	<-2 to -5

enriched beyond Oxic A (Figure 3.12).

When these differences were considered more generally, as major enrichment category discrepancies, the relative limitations in the sulfide based system were highlighted (Table 3.5). Regardless of the 32% classification agreement, even with the additional 17% that were classified within the same major enrichment category (Residual 0; Table 3.5), the sulfide based system was only able to match the VBH classification in oxic conditions except for one case where hypoxia was estimated. More notably is that 14 of the 15 visually hypoxic stations were associated with mean sulfide concentrations <1500 μM (Table 3.5); that is, 93% of all visually hypoxic stations included in this data set were being classified as oxic by current EMP practices. This is likely due to the sub-oxic zone, defined by low to no dissolved oxygen and low dissolved sulfide concentrations, being present at the sediment-water interface and captured during grab sample collections. Meanwhile, current threshold definitions suggest that intermediate sulfide concentrations (approximately 1500 μM) are present in the upper range of the oxygenated condition. This is based on an empirical relationship that assumes a gradual build up of sulfide from one enrichment category to the next (Hargrave et al., 2008), not factoring in the full extent to which sulfide may be sequestered in the transitory environments (Jørgensen, 1977; Berner, 1980; Preisler et al., 2007). For instance, the presence of intermediate oxidants (Berner, 1981a), and anaerobic chemical and biological oxidation and sequestration reactions with metal oxides/hydroxides (Preisler et al., 2007) and *Beggiatoa spp.* (Nelson et al., 1986) may result in a physical separation of oxygenated (>1 μM; O_2) and sulfidic (>1 μM; S^{2-}) sediments (Berner, 1981a, 1980; Preisler et al., 2007). Additionally, the homogenization of the sediment samples prior to measurement in the current system removes the ability to capture subtleties in the chemoclines, and therefore may result in falsily oxic classifications using the Hargrave et al. (2008), S^{2-} thresholds.

The largest residual differences are associated with visually anoxic conditions being

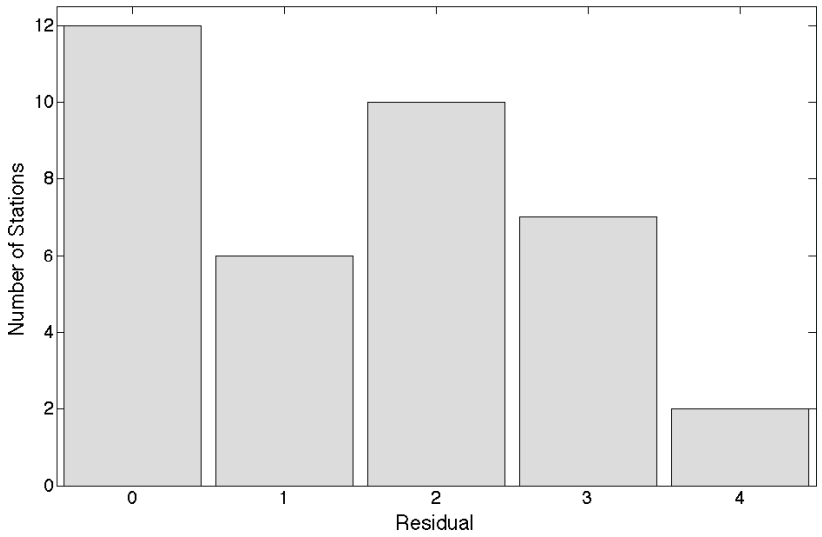

Figure 3.12: VBH - Sulfide rank residuals showing the number of stations that are in agreement (0) and the number of stations that are not (1-4).

connected with $<$1500 μM, total S^{2-} concentrations (Table 3.5). Three stations, one from each: Site E, Site B, and Site D, were defined in this group. The stations from Site B and Site D had *Beggiatoa* covering $>$60% and approximately 300 and 1000 μM of total S^{2-}, respectively. These sulfide concentrations are within the detectable range of the Orion electrode ($>$50 μM) and therefore suggest that sulfate reduction is actively producing sulfide in the surface sediments. Oremland and Polcin (1982) have found that methanogenesis and sulfate reduction can occur simultaneously in estuarine sediments, and this may explain why both outgassing and sulfide were observed at these stations. Alternatively, the Site E station had 1-29% mat cover and a $<$20 μM sulfide concentration. With regards to the detectable range of the Orion electrode, this station was effectively non-sulfidic and therefore likely methanic.

Visual based benthic health classification: With and without SPI

Finally, to explore the ability of visual based classification systems to extend into sandier environments, the same 37 stations were used to compare the Surface Index rankings to the VBH rankings. Again, two enrichment classifications ranging from 1 to 5 were assigned to each station based on the scaled index values in Table 3.4. These were then used to generate residuals by subtracting the Surface Index rankings from the VBH rankings.

Residuals indicated that 22 of the 37 stations were ranked as the same level of enrichment

Table 3.5: Major enrichment category discrepancies from the VBH index to mean sulfide concentration classification comparison.

Residual	Major enrichment Category	Number of Stations	Percentage (%)
0	Agreement	12	32
	Oxic	5	14
	Hypoxic	1	3
1	Hypoxic v Oxic	14	38
	Anoxic v Hypoxic	2	5
2	Anoxic v Oxic	3	8

by the two indices, and that the remaining 15 stations were only off by one enrichment category. Six of 15 were ranked higher by the Surface Index and the remaining nine were ranked higher by the VBH. Even though most stations were classified at the same level of enrichment, the slope of a simple linear regression of the two enrichment classifications suggest that the incorporation of SPI results in a more conservative ranking than when surface video is used alone (0.7435 $<$1; Figure 3.13). Regardless, good agreement (R^2=0.80821; n=37) between the methods suggest both the Surface Index and the VBH are able to define enrichment to a similar degree.

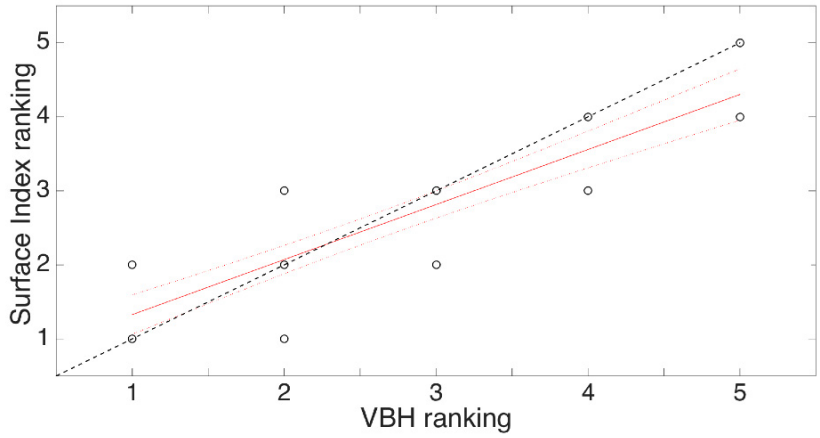

Figure 3.13: Simple linear regression of Surface Index rankings and VBH rankings calculated from the same visual data. Least squares regression line (solid red line) with 95% confidence intervals: y = 0.744x + 0.584; R^2 = 0.808, and a 1:1 ratio (dashed line) are also shown.

3.4 Discussion

The proposed classification systems offered here are solely based on defining the oxic condition of sediments as determined by visual biochemical and geochemical proxies. No direct oxygen measurements or macrofaunal assays were used. Although the inclusion of these measurements would have provided further support of the index parameters, there was no attempt to include them. Instead, indirect proxies with known sensitivities to increasingly oxic and/or sufidic conditions were used. Namely, the depth of the visual RPD boundary in surface sediments, which, due to it sensitivity, is susceptible to deepen when oxidized (Jørgensen, 1977; Otero et al., 2006) and to shallow when exposed sulfide, was included. Also considered was the *Beggiatoa spp.* behaviour to opposing oxygen and sulfide gradients (Møller et al., 1985; Nelson et al., 1986). These two formations were able to explain 73% and 66% of the VBH index variability, respectively.

Visual Benthic Health index

The VBH index was designed in light of existing indices that also employed SPI for benthic health assessments; the Benthic Health Quality index (BHQ; Nilsson and Rosenberg, 1997) and the Organism Sediment Index (OSI; Rhoads and Germano, 1986). A common feature in all three indices is the mean depth of the aRPD. This visual transition has been considered widely in the literature as an integrative proxy of sediment redox state (Nilsson and Rosenberg, 1997; Rhoads and Germano, 1986; Gerwing et al., 2013; Rosenberg et al., 2001) and therefore, is associated with positive index values that increase, asymptotically, with depth.

All three indices also include macrofaunal features as positive indicators of benthic health; however they differ in identification and value. The VBH is based on the presence/absence of the various features regardless of their relative abundance. This is different from the other indices; the BHQ index makes a distinction based on the number or size of parameters to determine whether more or less points are assigned to the overall score (Nilsson and Rosenberg, 1997), and the OSI, where values are based on identifying macrofauna succession (Rhoads and Germano, 1986). Regardless, the VBH applied a similar weighting approach as the BHQ index where oxidizing activities were valued higher than indicators of oxygenation. For example, epifaunal cues such as faecal pellets (in the BHQ) or benthic fish (in the VBH) are weighted less than infaunal or bioirrigating parameters

such as feeding pits or mounds (Nilsson and Rosenberg, 1997). Also, while successional stage is not consider in the VBH or BHQ, the VBH does incorporate multiple faunal groups (i.e. echinoderms, tube dwellers, crustaceans, etc.) to allow for a level of biodiversity to be included without formal measurement.

The most notable difference in the indices is the inclusion of negative values in both the VBH and OSI, that were not included in the BHQ. These were assigned to reducing parameters, such as outgassing or the presence of methane (VBH/OSI), and indicators of reduced conditions at the sediment surface, such as percent cover of *Beggiatoa spp.* (VBH). Considering *Beggiatoa* is unique to the VBH; however, it has been discussed in the literature as a candidate for indicating reducing conditions (Hamoutene et al., 2013; Hamoutene, 2014). For instance, Hamoutene et al. (2013) concluded that *Beggiatoa* presence was independent of depth and substrate type in a technical report based on work conducted around aquaculture sites in Newfoundland, Canada.

Beggiatoa and aRPD

Even though the *Beggiatoa* mat coverage and the aRPD depth are not independent of eachother (R^2=0.71) they did correlate well with the expected enrichment responses published in the literature. For instance, despite the majority of the stations having aRPD at 0 or >5 cm depth, the intermediate depth ranges were able to significantly reflect the enrichment gradient described in Pearson and Rosenberg (1978) general model of succession (R^2=0.73, $p<0.05$). Similarly, the observed *Beggiatoa spp.* response to the enrichment gradients in this study can be significantly described by the theoretical bell curve density distributions found in Preisler et al. (2007) and Weston (1990). The statistical uncertainty surrounding these two variables is attributed to the inclusion of other positive and negative parameters in the index. As a result, the use of multiple parameters integrated into a single VBH score resulted in a greater number of enrichment categories being defined at each depth or coverage range than if the aRPD or *Beggiatoa* were considered alone.

Other studies have found extensive *Beggiatoa* coverage to coincide with S^{2-} concentrations >3000 μM (Hargrave, 1993; Hamoutene, 2014; Brooks and Mahnken, 2003). By current threshold definitions, these are hypoxic conditions (Hargrave et al., 2008). In the same way, the only three stations from the present study that had sulfide concentrations >1500 μM also had >60% mat coverage. However, two of these three stations were

ranked as anoxic with the VBH due to gas bubbles being present at the sediment surface. More importantly, all other stations that had >60% *Beggiatoa* coverage were associated with an average total S^{2-} concentration of 396 $\pm$ 456.8 μM, much lower than those found in previous studies.

Also, it is important to note that the scenarios considered for mat coverage in the index are limited to assumptions based on the relative availability of dissolved oxygen and diffuse sulfide required to satisfy *Beggiatoa's* metabolic needs (Møller et al., 1985; Preisler et al., 2007; Nelson et al., 1986). However, patchy mat cover may also be attributed to storm events, where benthic re-suspension exposes surface sediments that were previously colonized by *Beggiatoa* to oxic bottom waters (Grant and Bathmann, 1987). Although the integrative nature of the visual redox boundary will likely remain representative of the pre-storm condition, unlikely to respond to short-term storm irrigation (Jørgensen, 1977), the removal or disturbance of mat cover could result in over- or underestimations of redox state. More detailed investigations are needed to examine the variability of surrounding *Beggiatoa* responses to storms, for example how long after storm events will it take mat coverage to return to stable pre-storm conditions. Until then, it is recommended that sampling wait at least 4 days after a storm event to allow for some recovery.

Enrichment classification systems

As a result of the visual data being collected alongside the NSDFA summer EMP sediment collections, the VBH classification system was able to be directly compared to the current sulfide based system. Differences between the systems were immediately identified since 46% of the 37 stations were defined as oxic using the visual thresholds opposed to the 91% of being classified as oxic using sulfide concentration. This 45% difference may be a result of how these thresholds are being defined. Hypoxic is defined in Hargrave et al. (2008) nomogram as >1500 μM of dissolve sulfide and <0.5 mg O_2 l^{-1}. This differs from Berner's definition where the transitory condition between oxygenated and polluted conditions are characterized by undetectable concentrations of both sulfide and oxygen. In 1981, Berner proposed a method for classify the diagenic succession in sedimentary environments based on the presence or absence of dissolved oxygen and dissolved sulfide. He categorized sediments as being either oxic or anoxic depending on whether dissolved oxygen was present in measurable concentrations (>1μM). The anoxic environments were then divided into sulfidic or non-sulfidic (i.e. post-oxic or methanic) depending on the

presence or absence of S^{2-}. Even though Berner (1981a) does not follow the oxic, hypoxic, anoxic enrichment categories of Hargrave et al. (2008), paralleled levels of succession were termed oxic, post-oxic, and sulfidic. Therefore it is speculated here that the overlap of oxygenated and sulfidic conditions in Hargrave et al.'s nomogram may be a potential explanation for why the visual based classification resulted in 45% more stations being defined as non-oxic.

This speculation was supported by the results presented in this study. It was suggested that the non-sulfidic, anaerobic conditions, defined by variables in the VBH index, were being misclassified with the use of current sulfide concentration thresholds alone. In fact, 93% of the 15 visually hypoxic stations were found associated with $<$1500 μM S^{2-} and therefore being classified as oxic with current EMP thresholds. Again, this is likely due to the sub-oxic condition not being fully considered in current thresholds. The sulfide ranges used to define the five enrichment categories are based on an empirical relationship that assume a gradual accumulation of total S^{2-} from one diagenic state to the next, more reduced, state (Hargrave et al., 2008). Another explanation has also been considered that suggests the homogenization of sediment samples, during sulfide analysis, is likely resulting in underestimations of pore-water concentrations at the 2 cm depth. Therefore, the low sulfide concentrations observed may not only be due to the sub-oxic regions being captured in the sediment samples, but also, whatever chemocline does exist, is likely being lost during analysis.

Similarly, three stations in the present study were ranked as visually anoxic with sulfide concentrations $<$1500 μM. All of these were coupled with gas bubbles being released from the surface sediments. In the work of Oremland and Polcin (1982), a study of competitive and non-competitive substrates for methanogenesis and sulfate reduction, it was concluded that methanogens are able to function in sulfate containing sediments by utilizing non-competitive compounds like methanol, trimethlamine, or methionine. Therefore, it has been speculated here that the two stations that had sulfide concentrations $>$300 μM and *Beggiatoa* mat coverage $>$30% may have been in non-competitive sediments where sulfate-reduction and methanogenesis were occurring simultaneously. However, one of the three stations had sulfide concentrations $<$20 μM and 1-29% mat coverage, suggesting methanic conditions, as defined in Berner (1981a), were present. Regardless, these visually anaerobic non-sulfidic conditions were again being classified as oxic.

A comparison of the VBH to the Surface Index was made to determine whether or not SPI limited the application of visual based classifications to muddy, muddy-sand environments (>35% porosity). Results suggest that both indices were able to define enrichment to a similar degree (R^2 = 0.808). However, the VBH was found to be generally more conservative in its ranking than the Surface Index, and therefore should be used when possible in order to adhere to the precautionary principle. Nevertheless, the good agreement of the two enrichment rankings suggests that visual based classifications can extend to sandier environments.

Conclusion

Benthic enrichment from aquaculture and similar types of organic eutrophication have been regarded as a leading global threat to coastal marine environments, demanding effective and efficient monitoring tools to measure and assess the associated impacts (Selman et al., 2008). For management purposes, enrichment thresholds are used to trigger mitigation strategies, such as fallowing, that are designed to recover the system back to a desired oxic state. In Nova Scotia, and many other coastal regions, total dissolved sulfide concentrations are used as a "sensitive" indicator in monitoring programs to infer the oxic condition. Even though there have been numerous attempts to standardize sulfide-measurement methodology in its application as a monitoring tool, little attention has been given to S^{2-} concentrations being a measure of toxicity (Grieshaber and Völkel, 1998) instead of its applied use as a proxy for the anaerobic condition. Although it is well established that total S^{2-} concentrations are low in the presence of dissolved oxygen (Thamdrup et al., 2000; Fenchel and Riedl, 1970; Jørgensen, 1977; Brooks and Mahnken, 2003; Berner, 1981b, 1980), there are also conditions where sulfide concentrations are low in the absence of dissolved oxygen (Preisler et al., 2007; Berner, 1981a).

The results of this study, in combination with previous reports (Berner, 1981a; Froelich et al., 1979; Emerson and Widmer, 1978; Mar), suggest the occurrence of anoxic, non-sulfidic environments are more common than previously recognized. Thus, when sulfide concentrations are used alone to define the oxic state, they are unable to differentiate between non-sulfidic aerobic conditions and non-sulfidic anaerobic conditions. That is why, in light of this study, it is recommended that visual based classification systems be used as a rapid and cost effective alternative for benthic enrichment assessments.

CHAPTER 4

CONCLUSION

Aquaculture practices are continuously evolving to try and become a more efficient and profitable industry. However, community and environmental stakeholders are still not convinced that this economic growth is without negative consequences to the local ecosystem. More effective monitoring practices are needed so that artificial eutrophication can be better managed; as a consequence, the social perception may also improve, reducing resistance against future development. Sedimentary conditions have long been considered a candidate for evaluating ecosystem health due to the stability of the conditions and integrative nature of biological, geochemical, and physical responses (Hargrave et al., 2008; Wildish et al., 1999, 2001; Brooks and Mahnken, 2003; Brooks et al., 2004; Grizzle and Penniman, 1991; Fenchel, 1969; Nilsson and Rosenberg, 1997, 2003). In general, oxic conditions in surface sediments are used to define low or no enrichment effects as these are the desired, if not stated, environmental quality objectives used in management efforts.

In Chapter 2, the aRPD was shown to be a viable proxy for redox state in soft-sediment, subtidal environments. This chapter also supported the use of SPI as a rapid and cost effective assessment tool that provides digitized visual images of undisturbed sub-surface conditions. Chapter 3 then applied the SPI and aRPD in a multi-parameter index, the Visual Benthic Health (VBH) index, that included other biological and geochemical cues. This was used to define visual based upper and lower hypoxic thresholds to be compared to those used in traditional sulfide based classification systems. The results suggested that the conventional methods were unable to distinguish between aerobic and anaerobic, non-sulfidic environments. For instance, current EMP practices, relying on concentrations of total dissolved sulfide, classified 91% of the 37 stations as oxic where the VBH only

classified 46% of the stations as oxic. Upon further investigation, 93% of visually hypoxic stations were found to be associated with $<$1500 μM S^{2-} concentrations. Despite the fact that this type of anaerobic, non-sulfidic environment has been described throughout the literature as a sub-oxic or post-oxic condition where well known geochemical boundaries (RPD) and microbial formations (i.e. *Beggiatoa spp.*) are found (Berner, 1981a; Hamoutene et al., 2013; Preisler et al., 2007; Froelich et al., 1979; Emerson and Widmer, 1978; Mar; Weston, 1990; Rosenberg et al., 2001), it had not been considered fully in the traditional definition of threshold boundaries. Similarly, three visually anoxic stations were classified as oxic with the sulfide based system. The presence of methane gas bubbles at all three of these stations suggest that low sulfides may be indicative of a methanic or grossly polluted system.

Results from this study also suggest that many stations were experiencing some degree of hypoxia, implying that further organic deposition would cause an increase in sulfide or methane concentration (Berner, 1981a). These reduced species present in the pore-water ultimately slow the recovery process back to the desired oxic state. Therefore, in order to effectively manage enrichment recovery, an early detection of the aerobic-anerobic transitions is essential. It is recommended that the VBH index be used under best management practices and adhere to the precautionary principle. However, if sediment type limits the penetration of SPI to depths $<$4 cm, an alternative visual based index, the Surface Index, was found to be a comparable method. The earlier identification of reducing conditions as a consequence of the indices will likely result in fewer leases becoming sulfidic/anoxic. Accordingly, mitigation strategies will be less expensive. For example, anoxic conditions may require many years ($>$3 years) of fallowing to return conditions back to acceptable levels (Specter and Specter, 2010), where as detecting hypoxic conditions before they become sulfidic may only require implementing reduced stocking densities and/or winter fallowing to allow for the natural seasonal irrigation (Jørgensen, 1977) to return the system back to acceptable conditions. In addition, the earlier implementation of mitigation stratigies will result aquaculture practices working close to, if not within, the natural oxic-hypoxic resilience of the system (Jørgensen, 1977). The reduced impacts to ecosystem health may in turn reduce social concerns and ultimately increase the sustainability of the industry.

Finally, even though these indices were designed to classify the level of enrichment

from aquaculture practices, similar types of organic eutrophication have been identified as leading global threats to coastal marine environments (Selman et al., 2008). Thus, the methods and techniques applied in this study can and should be considered for monitoring benthic conditions in response to other types of enrichment.

BIBLIOGRAPHY

Interstitial water chemistry of anoxic Long Island Sound sediments. 1. gases, author=Martens, Christopher S and Berner, Robert A, journal=Limnol. Oceanogr, volume=22, number=1, pages=10–25, year=1977.

Bagarinao, T., and I. Lantin-Olaguer, 1998. The sulfide tolerance of milkfish and tilapia in relation to fish kills in farms and natural waters in the Philippines. *Hydrobiologia*, **382**: 137–150.

Berner, R., 1979. *Principles of chemical sedimentology*, Mcraw-Hill, New York.

Berner, R. A., 1980. *Early diagenesis: A theoretical approach*, 1, Princeton University Press.

Berner, R. A., 1981a. A new geochemical classification of sedimentary environments. *Journal of Sedimentary Research*, **51**.

Berner, R. A., 1981b. Authigenic mineral formation resulting from organic matter decomposition in modern sediments. *Fortschritte der Mineralogie*, **59**: 117–135.

Berner, R. A., 1984. Sedimentary pyrite formation: An update. *Geochimica et Cosmochimica Acta*, **48**: 605–615.

Bertics, V. J., and W. Ziebis, 2010. Bioturbation and the role of microniches for sulfate reduction in coastal marine sediments. *Environmental Microbiology*, **12**: 3022–3034.

Boudreau, B. P., et al., 2005. Bubble growth and rise in soft sediments. *Geology*, **33**: 517–520.

Brooks, K. M., and C. V. Mahnken, 2003. Interactions of Atlantic salmon in the Pacific Northwest. II. Organic wastes. *Fish. Res.*, **60**: 255–293.

Brooks, K. M., A. R. Stierns, and C. Backman, 2004. Seven year remediation study at the Carrie Bay Atlantic salmon (Salmon salar) farm in the Broughton Archipelago, British Columbia, Canada. *Aquaculture*, **239**: 81–123.

Canfield, D. E., 1994. Factors influencing organic carbon preservation in marine sediments. *Chemical Geology*, **114**: 315–329.

Carlsson, M. S., P. Engström, O. Lindahl, L. Ljungqvist, J. K. Petersen, L. Svanberg, and M. Holmer, 2012. Effects of mussel farms on the benthic nitrogen cycle on the Swedish west coast. *Aquaculture Environment Interactions*, **2**: 177–191.

Carroll, M. L., S. Cochrane, R. Fieler, R. Velvin, and P. White, 2003. Organic enrichment of sediments from salmon farming in Norway: Environmental factors, management practices, and monitoring techniques. *Aquaculture*, **226**: 165–180.

Claypool, G. E., and I. Kaplan, 1974. The origin and distribution of methane in marine sediments, in *Natural gases in marine sediments*, pp. 99–139, Springer.

Coggan, R., J. Populus, J. White, K. Sheehan, F. Fitzpatrick, and S. Piel, 2007. Review of standards and protocols for seabed habitat mapping. *Mapping European Seabed Habitats (MESH), Peterborough, UK*.

Curtis, C., R. Burns, and J. Smith, 1977. Sedimentary geochemistry: Environments and processes dominated by involvement of an aqueous phase [and discussion]. *Philosophical Transactions of the Royal Society of London. Series A, Mathematical and Physical Sciences*, **286**: 353–372.

De Wit, R., H. M. Jonkers, F. P. Van Den Ende, and H. Van Gemerden, 1989. *In situ* fluctuations of oxygen and sulphide in marine microbial sediment ecosystems. *Netherlands Journal of Sea Research*, **23**: 271–281.

Emerson, S., and G. Widmer, 1978. Early diagenesis in anaerobic lake sediments II. Thermodynamic and kinetic factors controlling the formation of iron phosphate. *Geochimica et Cosmochimica Acta*, **42**: 1307–1316.

Fenchel, T., 1969. The ecology of marine microbenthos. IV. Structure and function of the benthic ecosystem, its chemical and physical factors and the microfauna communities with special reference to ciliated Protozoa. *Ophelia*, **6**: 1–182.

Fenchel, T., and R. Riedl, 1970. The sulfide system: A new biotic community underneath the oxidized layer of marine sand bottoms. *Marine Biology*, **7**: 255–268.

Finke, N., V. Vandieken, and B. B. Jørgensen, 2007. Acetate, lactate, propionate, and isobutyrate as electron donors for iron and sulfate reduction in Arctic marine sediments, Svalbard. *FEMS Microbiology Ecology*, **59**: 10–22.

Fisheries and Oceans, 2010. Aquaculture Canada: Fact and figures.

Froelich, P. N., et al., 1979. Early oxidation of organic matter in pelagic sediments of the eastern equatorial Atlantic: Suboxic diagenesis. *Geochimica et Cosmochimica Acta*, **43**: 1075–1090.

Gerwing, T. G., A. M. A. Gerwing, D. Drolet, D. J. Hamilton, and M. A. Barbeau, 2013. Comparison of two methods of measuring the depth of the redox potential discontinuity in intertidal mudflat sediments. *Marine Ecology Progress Series*, **487**: 7–13.

Giles, H., 2008. Using Bayesian networks to examine consistent trends in fish farm benthic impact studies. *Aquaculture*, **274**: 181–195.

Grant, J., 2010. Coastal communities, participatory research, and far-field effects of aquaculture. *Aquaculture Environment Interactions*, **1**: 85–93.

Grant, J., and U. V. Bathmann, 1987. Swept away: Resuspension of bacterial mats regulates benthic-pelagic exchange of sulfur. *Science*, **236**: 1472–1474.

Gray, J., R. Wu, and Y. Or, 2002. Effects of hypoxia and organic enrichment on the coastal marine environment. *Marine Ecology Progress Series*, **238**: 249–279.

Grieshaber, M. K., and S. Völkel, 1998. Animal adaptations for tolerance and exploitation of poisonous sulfide. *Annual review of physiology*, **60**: 33–53.

Grizzle, R., and C. Penniman, 1991. Effects of organic enrichment on estuarine macrofaunal benthos: A comparison of sediment profile imaging and traditional methods. *Marine Ecology Progress Series MESEDT,*, **74**.

Hamoutene, D., 2014. Sediment sulphides and redox potential associated with spatial coverage of Beggiatoa spp. at finfish aquaculture sites in Newfoundland, Canada. *ICES Journal of Marine Science: Journal du Conseil*, p. fst223.

Hamoutene, D., G. Mabrouk, L. Sheppard, C. MacSween, E. Coughlan, and C. Grant, 2013. Validating the use of Beggiatoa sp. and opportunistic polychaete worm complex (OPC) as indicators of benthic habitat condition at finfish aquaculture sites in Newfoundland. *Canadian Technical Report of Fisheries and Aquatic Sciences 3028, vii. 18pp*.

Hansen, P. K., A. Ervik, M. Schaanning, P. Johannessen, J. Aure, T. Jahnsen, and A. Stigebrandt, 2001. Regulating the local environmental impact of intensive, marine fish farming: Ii. the monitoring programme of the MOM system (Modelling–Ongrowing fish farms–Monitoring). *Aquaculture*, **194**: 75–92.

Hargrave, B., 1993. Seasonal changes in benthic fluxes of dissolved oxygen and ammonium associated with marine cultured Atlantic Salmon. *Mar. Ecol. Prog. Ser.*, **96**: 249–257.

Hargrave, B., 2010. Empirical relationships describing benthic impacts of salmon aquaculture. *Aquacult. Environ. Interact*, **1**: 33–46.

Hargrave, B. T., M. Holmer, and C. P. Newcombe, 2008. Towards a classification of organic enrichment in marine sediments based on biogeochemical indicators. *Marine Pollution Bulletin*, **56**: 810–824.

Howarth, R. W., 1979. Pyrite: Its rapid formation in a salt marsh and its importance in ecosystem metabolism. *Science*, **203**: 49–51.

Jørgensen, B. B., 1977. The sulfur cycle of a coastal marine sediment (Limfjorden, Denmark). *Limnol. Oceanogr*, **22**: 814–831.

Jørgensen, B. B., and T. Fenchel, 1974. The sulfur cycle of a marine sediment model system. *Marine Biology*, **24**: 189–201.

Karakassis, I., M. Tsapakis, C. J. Smith, and H. Rumohr, 2002. Fish farming impacts in the Mediterranean studied through sediment profiling imagery. *Marine Ecology Progress Series*, **227**: 125–133.

Le Hir, P., W. Roberts, O. Cazaillet, M. Christie, P. Bassoullet, and C. Bacher, 2000. Characterization of intertidal flat hydrodynamics. *Continental Shelf Research*, **20**: 1433–1459.

Lyle, M., 1983. The brown-green color transition in marine sediments: A marker of the fe (iii)-fe (ii) redox boundary [iron (iii)-iron (ii)]. *Limnology and Oceanography*.

Middleburg, J., C. Duarte, and J. Gattuso, 2005. Respiration in coastal benthic communities, in *Respiration in aquatic ecosystems: History and background*, edited by P. l. B. Williams and P. A. del Giorgio, pp. 206–224, Oxford University Press, Oxford.

Milewski, I., 2013. Aquaculture survey and macro-invertebrate analysis report: 2013 Sandy Point survey, Shelburne Harbour (Nova Scotia). *Conservation Council of New Brunswick*.

Møller, M. M., L. P. Nielsen, and B. B. Jørgensen, 1985. Oxygen responses and mat formation by Beggiatoa spp. *Applied and Environmental Microbiology*, **50**: 373–382.

Mulsow, S., Y. Krieger, and R. Kennedy, 2006. Sediment profile imaging (SPI) and micro-electrode technologies in impact assessment studies: Example from two fjords in southern chile used for fish farming. *Journal of Marine Systems*, **62**: 152–163.

Nelson, D. C., B. B. Jørgensen, and N. P. Revsbech, 1986. Growth pattern and yield of a chemoautotrophic Beggiatoa sp. in oxygen-sulfide microgradients. *Applied and Environmental Microbiology*, **52**: 225–233.

Nilsson, H., and R. Rosenberg, 1997. Benthic habitat quality assessment of an oxygen stressed fjord by surface and sediment profile images. *Journal of Marine Systems*, **11**: 249–264.

Nilsson, H. C., and R. Rosenberg, 2000. Succession in marine benthic habitats and fauna in response to oxygen deficiency: Analysed by sediment profile-imaging and by grab samples. *Marine Ecology Progress Series*, **197**: 139–149.

Nilsson, H. C., and R. Rosenberg, 2003. Effects on marine sedimentary habitats of experimental trawling analysed by sediment profile imagery. *Journal of Experimental Marine Biology and Ecology*, **285**: 453–463.

NSDFA, 2014a. Environmental monitoring program framework for marine aquaculture in Nova Scotia. *Nova Scotia Aquaculture Environmental Monitoring Program*.

NSDFA, 2014b. Standard operating procedures for the environmental monitoring of marine aquaculture in nova scotia. *Nova Scotia Aquaculture Environmental Monitoring Program*.

Oremland, R. S., and S. Polcin, 1982. Methanogenesis and sulfate reduction: Competitive and noncompetitive substrates in estuarine sediments. *Applied and Environmental Microbiology*, **44**: 1270.

Otero, X. L., R. M. Calvo de Anta, and F. Macıas, 2006. Sulphur partitioning in sediments and biodeposits below mussel rafts in the rıa de arousa (galicia, nw spain). *Marine environmental research*, **61**: 305–325.

Pearson, T., and R. Rosenberg, 1978. Macrobenthic succession in relation to organic enrichment and pollution of the marine environment. *Oceanogr. Mar. Biol. Ann. Rev*, **16**: 229–311.

Preisler, A., D. De Beer, A. Lichtschlag, G. Lavik, A. Boetius, and B. B. Jørgensen, 2007. Biological and chemical sulfide oxidation in a Beggiatoa inhabited marine sediment. *The ISME journal*, **1**: 341–353.

Rhoads, D. C., 1974. Organism-sediment relations on the muddy sea floor. *Mar. Biol. Ann. Rev.*, **12**: 263–300.

Rhoads, D. C., and S. Cande, 1971. Sediment profile camera for in situ study of organism-sediment relations. *Limnology and Oceanography*, pp. 110–114.

Rhoads, D. C., and J. D. Germano, 1982. Characterization of organism-sediment relations using sediment profile imaging: An efficient method of remote ecological monitoring of the seafloor(REMOTS (TM) system). *Marine Ecology Progress Series. Oldendorf*, **8**: 115–128.

Rhoads, D. C., and J. D. Germano, 1986. Interpreting long-term changes in benthic community structure: A new protocol. *Hydrobiologia*, **142**: 291–308.

Rosenberg, R., H. C. Nilsson, and R. J. Diaz, 2001. Response of benthic fauna and changing sediment redox profiles over a hypoxic gradient. *Estuarine, Coastal and Shelf Science*, **53**: 343–350.

Selman, M., S. Greenhalgh, R. Diaz, and Z. Sugg, 2008. Eutrophication and hypoxia in coastal areas: A global assessment of the state of knowledge. *World Resources Institute*, **284**.

Specter, M., and H. Specter, 2010. Environmental assessment: CEAR Reference 10-01-54213.

Thamdrup, B., and D. E. Canfield, 2000. Benthic respiration in aquatic sediments, in *Methods in Ecosystem Science*, pp. 86–103, Springer.

Thamdrup, B., R. Rosselló-Mora, and R. Amann, 2000. Microbial manganese and sulfate reduction in Black Sea shelf sediments. *Applied and Environmental Microbiology*, **66**: 2888–2897.

Valente, R. M., D. C. Rhoads, J. D. Germano, and V. J. Cabelli, 1992. Mapping of benthic enrichment patterns in Narragansett Bay, Rhode Island. *Estuaries*, **15**: 1–17.

Van Hoey, G., S. N. Birchenough, and K. Hostens, 2014. Estimating the biological value of soft-bottom sediments with sediment profile imaging and grab sampling. *Journal of Sea Research*, **86**: 1–12.

Weston, D. P., 1990. Quantitative examination of macrobenthic community changes along an organic enrichment gradient. *Marine Ecology Progress Series. Oldendorf*, **61**: 233–244.

Wildish, D., B. Hargrave, and G. Pohle, 2001. Cost-effective monitoring of organic enrichment resulting from salmon mariculture. *ICES Journal of Marine Science: Journal du Conseil*, **58**: 469–476.

Wildish, D. J., H. M. Akagi, N. Hamilton, and B. T. Hargrave, 1999. A recommended method for monitoring sediments to detect organic enrichment from mariculture in the Bay of Fundy. *Canadian technical report of fisheries and aquatic sciences/Rapport technique Canadien des sciences halieutiques et aquatiques. Imprint varies*, **2286**: 34.

APPENDIX A

LABORATORY TECHNIQUES

A.0.1 Redox Potential

24 hours in advance

- Fill an oxidation reduction potential (ORP) Pt electrode (e.g. Orion 96-78NWP) with 4M KCl saturated with Ag/AgCl (e.g. Orion solution # 900011)

Right before

- Assess electrode performance with ORP Standard (Orion 967901) solution to the bottles specification (+220 $\pm$ 3 mV at 25°C)
- The ORP electrode and temperature probe are inserted into the sampling vial and the stabilized mV reading (stabilized in $\pm$ 10 mV or whatever the reading is after 2 min) and temperature are recorded (NSDFA, 2014b). The millivolt readings are then corrected to the normal hydrogen electrode (Eh_{NHE}) using the equation A.1

$$Eh_{NHE} = E_0 + (224 - T) \tag{A.1}$$

where E_0 is the mV reading of the unknown and T is the temperature of the unknown in °C (NSDFA, 2014b). The electrode is rinsed with distilled water and dried after every reading.

A.0.2 Sulfide Concentration

Materials

24 hours in advance

- Fill a Ag^{+}/S^{2-} combination electrode (e.g. Orion # 96-16BNWP) with Optimum Results^{TM} A solution (Orion # 900061).

- Prepare de-oxygenated distilled (DD) water by boiling distilled water.
- Prepare 500 mL of sulfide anti-oxidant buffer (SAOB) solution by diluting 40.0g of NaOH and 35.8g of EDTA buffer (ethylenediaminetetraacetic acid disodium salt dehydrate) with DD water.

Right before

- Prepare buffer solution by mixing 3.85g L-Ascorbic Acid (L-aa) with 110 mL SAOB.
- Prepare an initial 0.04288M Na_2S stock solution by weighing out 1.030g $Na_2S \times$ 9H2O into a 100 mL volumetric flask. To create a five-point concentration series follow the solution preparation guidelines (Table A.1) diluting at each step with DD. 'Discarded volume' is meant to keep solutions at equal volume by the end of standard preparation.

Table A.1: Five-point serial dilution guidelines using 25 mL volumetric flasks.

Stock	Transfer volume (mL)	Concentration (μM)	Discard volume (mL)
Initial	5.83	10 000	-
10 000	12.50	5000	-
5000	5.00	1000	7.50
1000	12.50	500	-
500	5.00	100	7.50
100	0	100	12.50

- Calibrate the electrode to a five point standard curve using the known concentrations of the solutions prepared. Starting with the most dilute standard (100 μM), add 5 mL of the SAOB+L-aa (1:1 dilution) and mix well. Insert the electrode and temperature probe into the mixture until the reading stabilizes. Record this value next to the known ionic concentration along with the temperature at which the stabilized. Rinse electrode and temperature probe with distilled water and dry in between samples. Repeat for all five solutions recording the mV at the same temperature each time.
- After the redox value has been recorded an equal part of the pre-mixed SAOB+L-aa solution is then added into the sampling vial and mixed well. The Ag^{+}/S^{2-} electrode

and temperature probe are then inserted into the resulting sediment slurry and the mV reading is recorded at the temperature that the probe was calibrated. The curve is then used to interpolate the ionic concentration of the samples from the millivolt reading.

**NOTE: The electrode must be re-calibrated every 3 hours to account for time dependent drift in solutions used.

A.0.3 Porosity

Materials

24 hours in advance

- Preheat a gravity convection drying oven to 60°C

Deposit the sediment sample into a pre-weighed sampling vial. Record the wet weight (ww g) and place in the oven for 24 - 48 hours. Re-weigh the sample vial and record the dry weight (dw g). After subtracting the pre-weighed vial weight from each recording you can calculate the porosity as the percentage of water occupying the pore space in each sample.

$$Porosity = \frac{(ww - dw)}{ww} \times 100\% \tag{A.2}$$

A.0.4 Organic matter content

Materials

24 hours in advance

- Preheat muffle furnace to 490°C

After the samples have been analysed for porosity the sediment can be removed from the sample vials and ground with a mortar and pestle. Transfer the ground sediments to pre-weighed/labelled aluminum dishes. Record the dry weight (dw g) of the sediments in the aluminum dish and then place them in the muffle furnace for eight hours. Re-weigh the aluminum dishes and record the ashed weights (aw g) of the samples. After subtracting the pre-weighed dish weight from each recording you can calculate the organic content as the percentage of labile matter combusted in each sample.

$$Organic = \frac{(dw - aw)}{dw} \times 100\% \tag{A.3}$$